3-Acetyl-8-methoxy-2[H]-chromen-2-one derived Schiff bases as potent antiproliferative agents: Insight into the influence of 4(N)-substituents on the in vitro biological activity

G. Kalaiarasi, S. Rex Jeya Rajkumar, G. Aswini, S. Dharani, Frank R. Fronczek, R. Prabhakaran

PII: S1386-1425(18)30333-0
DOI: doi:10.1016/j.saa.2018.04.028
Reference: SAA 15985
To appear in: *Spectrochimica Acta Part A: Molecular and Biomolecular Spectroscopy*
Received date: 17 January 2018
Revised date: 11 April 2018
Accepted date: 13 April 2018

Please cite this article as: G. Kalaiarasi, S. Rex Jeya Rajkumar, G. Aswini, S. Dharani, Frank R. Fronczek, R. Prabhakaran , 3-Acetyl-8-methoxy-2[H]-chromen-2-one derived Schiff bases as potent antiproliferative agents: Insight into the influence of 4(N)-substituents on the in vitro biological activity. The address for the corresponding author was captured as affiliation for all authors. Please check if appropriate. Saa(2017), doi:10.1016/j.saa.2018.04.028

3-Acetyl-8-methoxy-2[H]-chromen-2-one derived Schiff bases as potent antiproliferative agents: Insight into the influence of 4(*N*)-substituents on the *in vitro* biological activity

G. Kalaiarasi,[a] S. Rex Jeya Rajkumar,[b] G. Aswini,[a] S. Dharani,[a] Frank R. Fronczek,[c] and R. Prabhakaran [a*]

[a] *Department of Chemistry, Bharathiar University, Coimbatore 641 046, India.*

[b] *Department of Biosciences and Technology, Karunya University, Coimbatore 641 114, India.*

[c] *Department of Chemistry, Louisiana State University, Baton Rouge, LA 70803, USA*

Abstract

A series of 3-acetyl-8-methoxycoumarin appended thiosemicarbazones (**1**-**4**) was prepared from the reaction of 3-acetyl-8-methoxycoumarin with 4(*N*)-substituted thiosemicarbazides in a view of ascertaining their biological properties with the change of *N*-terminal substitution in the thiosemicarbazide moiety. Comprehensive characterization was brought about by various spectral and analytical methods. The molecular structures of all the compounds were determined by single crystal X-ray diffraction analysis. Binding studies with Calf thymus DNA (CT-DNA) and proteins such as Bovine Serum Albumin (BSA) and Human Serum Albumin (HSA) indicated an intercalative mode of binding with DNA and static quenching mechanism with proteins. The compounds cleaved plasmid DNA (pBR322) and acted well as free radical scavengers. A good spectrum of antimicrobial activity was observed against four bacterial and five fungal pathogens. The compounds exhibited profound antiproliferative activity on MCF-7 (human breast cancer) and A549 (human lung carcinoma) cell lines. Assay on human normal keratinocyte cell line HaCaT showed that the compounds were non-toxic to normal cells.

Key words: Coumarin Schiff Bases; Spectroscopy; X-ray crystallography; DNA/protein binding; Antimicrobial studies; Anticancer activity.

Corresponding author *Tel.: +91-422-2428319; Fax: +91-422-2422387; E-Mail: rpnchemist@gmail.com* (R. Prabhakaran)

Introduction

The chemistry of heterocyclic compounds is always been a promising field of research, from which numerous applications could be accounted. Stemming from their pharmacological and physical properties, coumarins and their derivatives have emerged as attractive synthetic targets. A number of organic compounds containing this coumarin scaffold are reported to exhibit antidepressant [1], antitumor [2], anti-inflammation [3], antimicrobial [4], antiviral [5], anticoagulant properties [6] and found to inhibit Aβ peptide aggregation [7]. Substitution affects the activity of coumarin to a greater extent. For example, structure activity relationship studies denote that the presence of an alkyloxy group at 7^{th} position increases the potential to reduce plasma alkaline tranferase level in hepatitis and inhibition of caspase-3 activation [8]. In particular, 7-hydroxy-4-methyl coumarin derivatives possess varied biological properties including neuroleptic, antitubercular, anti-HIV, antimicrobial, antineoplastic and antihelmintic [9,10]. Coumarin derivatives target a number of pathways in cancer cells such as cell cycle arrest, antimitotic activity, inhibition of kinase, angiogenesis, heat shock protein (HSP90), telomerase, carbonic anhydrase, etc [11]. On the other hand, coumarin fused heterocycles exhibit unprecedented properties and function effectively as antioxidants [12]. More than 1300 coumarin derivatives have been identified till date [13]. A report on natural and synthetic coumarins made by Fylaktakidou *et al* [14] and Bansal *et al* [3] depicts their potential as anti-inflammatory and antioxidant agents. Zacharski *et al* demonstrated that warfarin ((RS)-4-hydroxy-3-(3-oxo-1-phenylbutyl)-2H-chromen-2-one), a coumarin containing compound, can prolong the survival of cancer patients [15]. These reports provide a comprehensive discussion on the importance of coumarin derivatives in the current research scenario. Moreover, condensation of substituted coumarins with thiosemicarbazides results in the enhancement of their biological activity [16]. As such, both the thiosemicarbazides and coumarins have their own capability in exhibition of pharmaceutical properties [17-20]. In order to get a deep insight into their biological activity, we made a systematic study on the derivatives of 3-acetyl-8-methoxycoumarin with four different substituted thiosemicabazides.

Results and Discussion

Synthesis and Characterization

The preparative route for 3-acetyl-8-methoxycoumarin-4(*N*)-substituted thiosemicarbazones (**1-4**) are given in Scheme 1 and formation of the compounds was confirmed by spectral techniques (IR, UV-Vis and ^{1}H NMR) and single crystal X-ray diffraction studies. The

compounds were stable to light and air and dissolve in common organic solvents such as methanol, acetonitrile, dichloromethane, chloroform, ethanol, dimethylformamide and dimethylsulfoxide. The compounds were stable in aqueous solutions, which was confirmed by using UV-Visible spectroscopic techniques (Fig. S1).

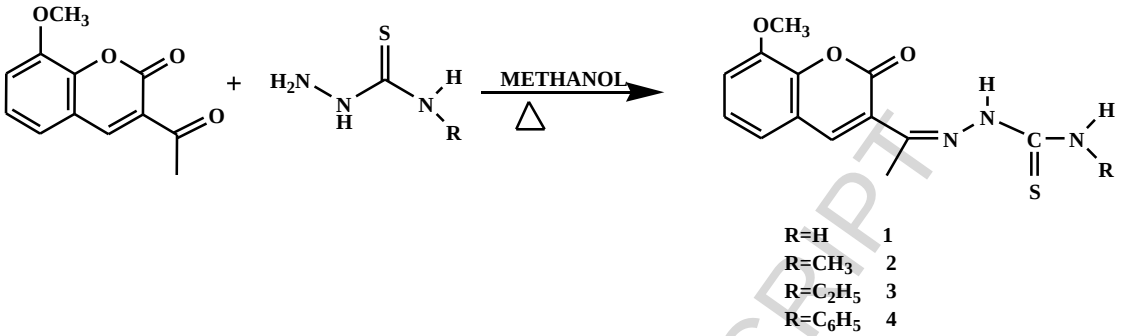

Scheme 1. Synthesis of the compounds (1-4)

Spectroscopic studies

The IR and UV-Visible spectral details have been discussed in the supporting information**.**

In the ^{1}H-NMR spectra of the compounds **1-4** (Fig. S2-S6), a signal appeared at δ 2.23-2.32 ppm due to the N=C-CH_3 proton [21] and a singlet observed at δ 10.32-10.86 ppm corresponding to the hydrazinic proton N(2)–H [22]. The signals due to C5, C6 and C7 protons appeared as a multiplet in the region of δ 7.15-7.59 ppm while the C4 proton accounted for a sharp signal centered at δ 7.95-8.47 ppm [23]. The signals due to –OCH_3 group protons observed as a singlet at δ 3.90 ppm [22] and NH_2 protons for **1** appeared as two broad singlet at δ 8.39 and δ 8.44 ppm. In the spectra of **2**, **3** and **4** the terminal –NH protons observed as a quartet, triplet and singlet at δ 8.48-8.51, δ 8.47-8.50 and δ 10.15 ppm respectively. The methyl group and methylene group of protons observed in the expected region.

X-Ray crystallography

The molecular structures of the compounds **1**–**4** have been determined by single crystal X-ray diffraction method and the ORTEP drawings are shown in Fig. 1-4. The details concerning the data collection and structure refinement of the compounds are summarized in Table 1 and selected bond distances and bond angles of the compounds **1**–**4** are given in Table S1 in the supporting information.

Crystal structure of compounds 1–4

The compounds **1** and **2** crystallized in monoclinic $P2_1/c$ (**1**), orthorhombic Pbca (**2**) space group respectively and triclinic symmetry with P-1 space group for the compounds **3** and **4**. The crystal structure of the compounds **1-4** showed that the thiocarbonyl sulphur (S1) and imine nitrogen N(1) atom in the thiosemicarbazone are *trans* to each other across the C(11)-N(2) bond. The structural arrangement corresponds to the *E*-isomer. The bond distances and bond angles in the compounds **1-4** agree well with the values observed for other reported Schiff bases and coumarin derivatives [21-26] where the C(11)=S(1) group found as thione form with the bond length of 1.6868(5) Å, 1.6847(10) Å, 1.6839(5) Å and 1.6813(11) Å for **1**, **2**, **3** and **4** respectively. Further, no large charge delocalization was detected.

In compound **1**, O(1) oxygen atom of the first molecule is engaged in intermolecular hydrogen bonding with one of the hydrogen atoms of the amino group of the second molecule O(1)…H(31)-N(3), whereas the O(3) oxygen atom of the first molecule is engaged in intermolecular hydrogen bonding with second hydrogen atom of the amino group in second molecule. In addition, the O(1) and O(3) oxygen atoms of the second molecule makes a bond with the hydrogen atoms of the amino group of the next molecule and this intermolecular hydrogen bonding at both the end led to a layer structure (Fig. 5; Table 2). In compound **3** we found the donor–acceptor distance (3.034 and 3.034 Å) corresponding to the N(1)-O(1) and O(1)-N(1) bond between the two molecules (Fig. 6; Table 2).

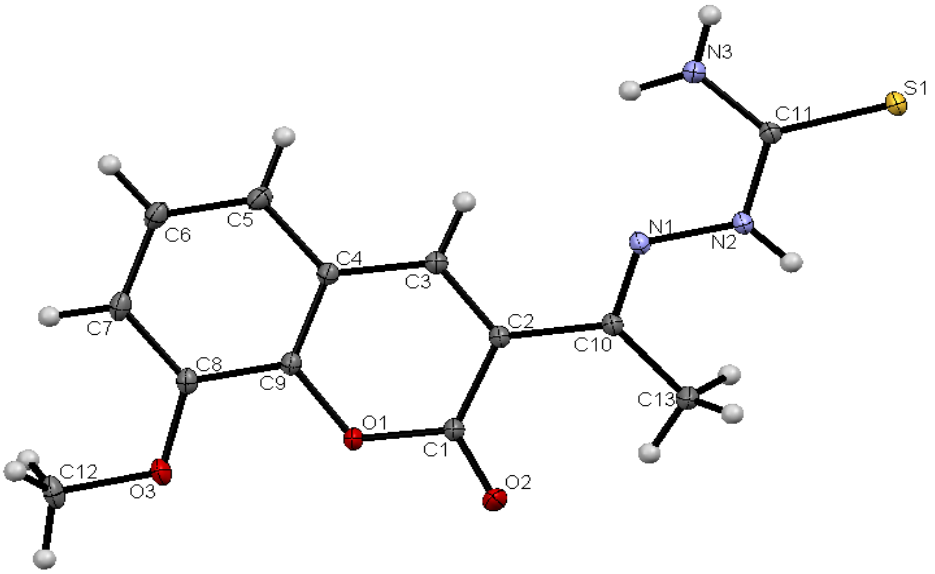

Fig. 1. ORTEP diagram of [8MAC-tsc)] (**1**) (thermal ellipsoid at 30% probability level)

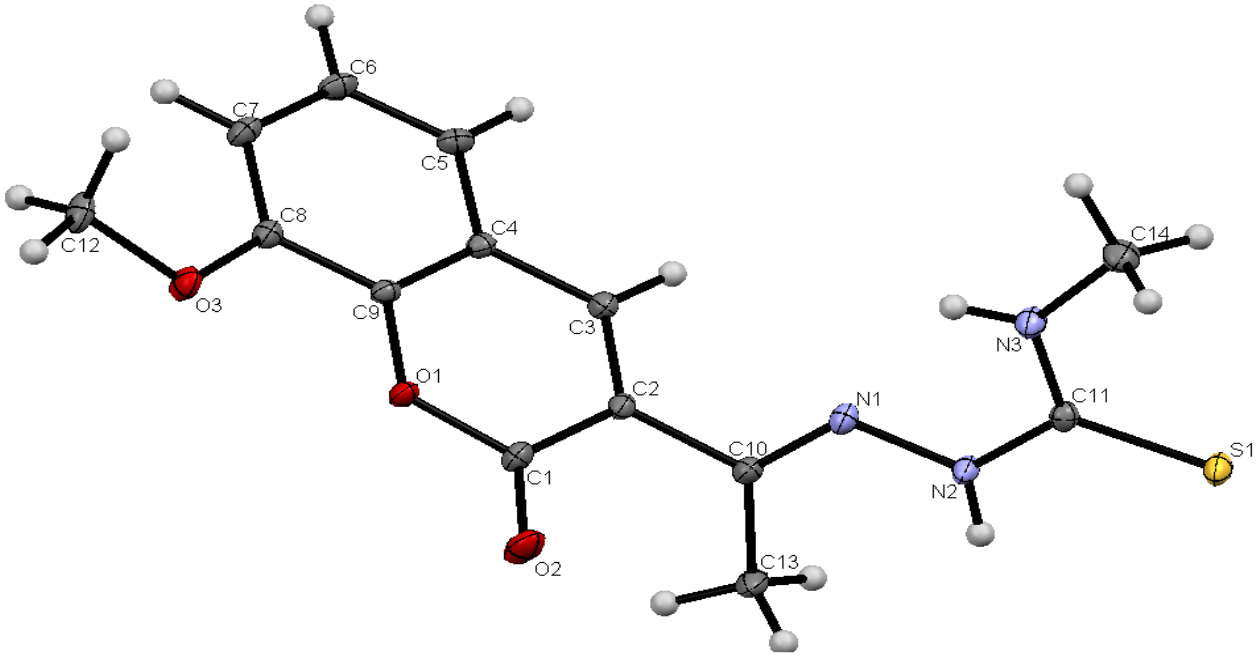

Fig. 2. ORTEP diagram of [8MAC-mtsc)] (**2**) (thermal ellipsoid at 30% probability level)

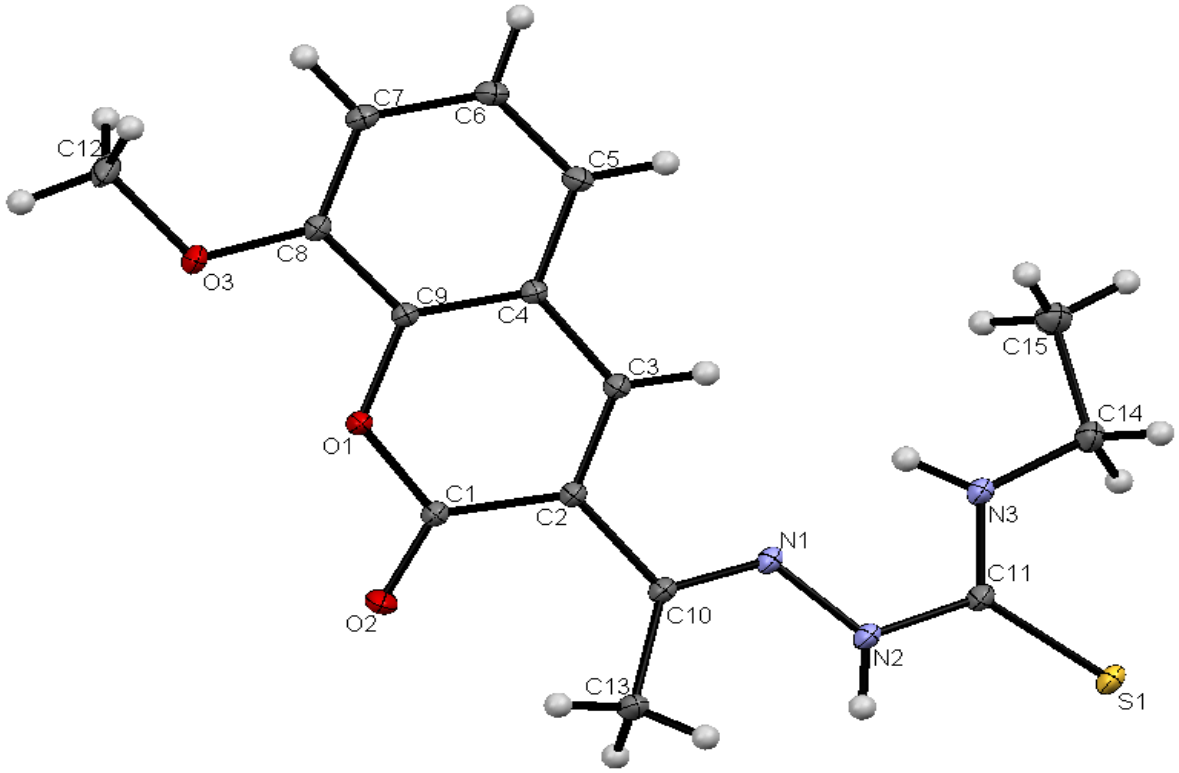

Fig. 3. ORTEP diagram of [8MAC-etsc)] (**3**) (thermal ellipsoid at 30% probability level)

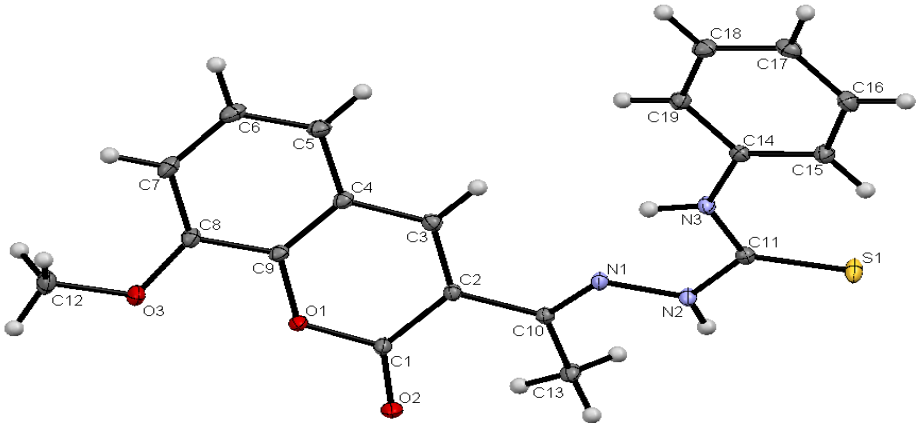

Fig. 4. ORTEP diagram of [8MAC-ptsc)] (**4**) (thermal ellipsoid at 30% probability level)

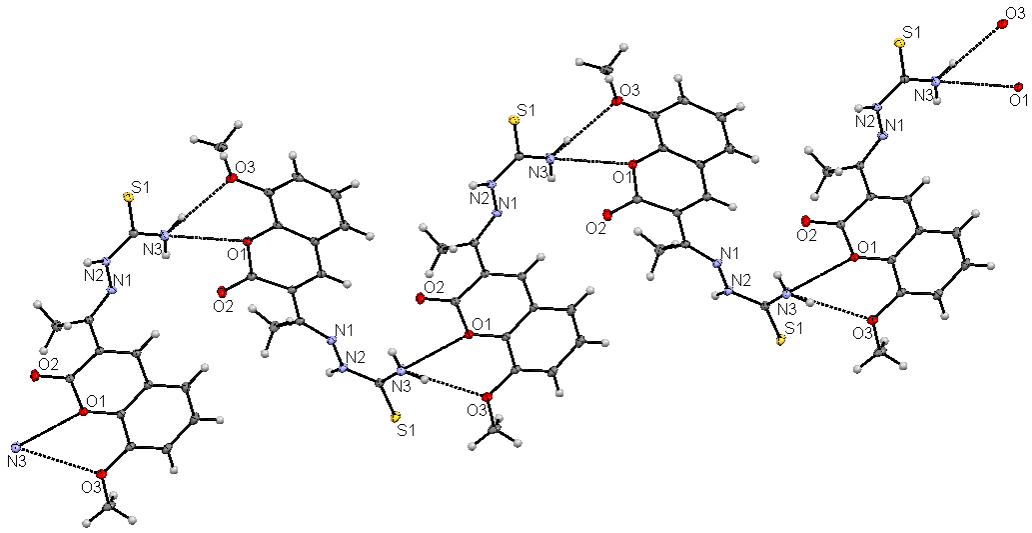

Fig. 5. ORTEP diagram of [8MAC-tsc)] (**1**) with hydrogen bonding

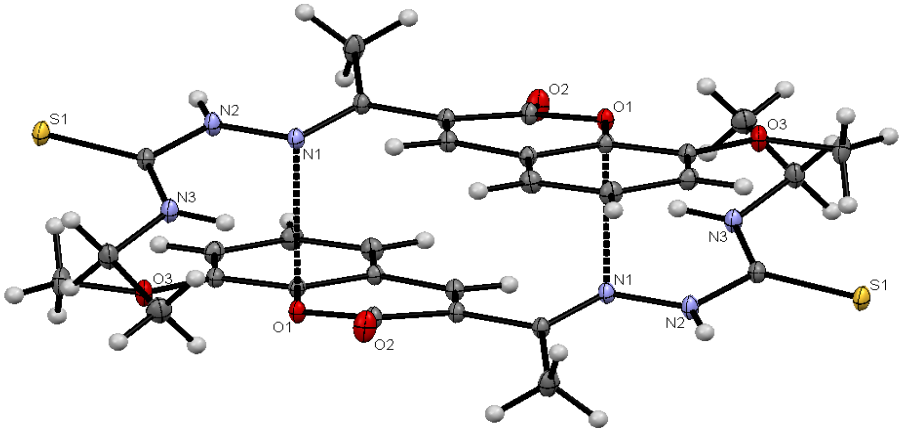

Fig. 6. ORTEP diagram of [8MAC-etsc)] (**3**) with hydrogen bonding

Table 1. Crystallographic data of the compounds **1-4**

Identification code	[8MAC-tsc)](**1**)	[8MAC-mtsc)](**2**)	[8MAC-etsc)] (**3**)	[8MAC-ptsc)](**3**)
Empirical formula	$C_{13}H_{13}N_3O_3S$	$C_{14}H_{15}N_3O_3S$	$C_{15}H_{17}N_3O_3S$	$C_{19}H_{17}N_3O_3S$
Formula weight	291.32	305.35	319.38	367.41
Temperature	90.0(5) K	90.0(5) K	90.0(5) K	90.0(5) K
Wavelength	0.71073 Å	0.71073 Å	0.71073 Å	0.71073 Å
Crystal system	Monoclinic	Orthorhombic	Triclinic	Triclinic
Space group	$P2_1/c$	P bca	P -1	P-1
Unit cell dimensions				
A	4.7341(18) Å	7.4705(2) Å	8.0293(3) Å	7.1312(4) Å
B	13.5129(5)Å	17.8863(6) Å	9.5230(4) Å	9.5534(4) Å
C	20.2518(8) Å	21.2458(7) Å	10.8690(4) Å	13.4948(6) Å
α	90°	90°	71.7983(18)°	107.481(2)°
β	96.2640 (18)°	90°	70.982(2)°	102.918(3)°
γ	90°	90°	73.884(2)°	94.324(3)°
Volume	1287.8 $Å^3$	2838.86 $Å^3$	731.96 $Å^3$	844.603 $Å^3$
Z	4	8	2	2
Density	1.503 Mg/m^3	1.429 Mg/m^3	1.449 Mg/m^3	1.445 Mg/m^3
Absorption coefficient,	0.263 mm^{-1}	0.242 mm^{-1}	0.238 mm^{-1}	0.217 mm^{-1}
F(000)	608	1280	336	384
Crystal size	0.33 × 0.26 × 0.25 mm^3	0.29 × 0.23 × 0.14 mm^3	0.33 × 0.25 × 0.19 mm^3	0.26 × 0.14 × 0.07 mm^3
θ range for data collection	1.815 to 40.27 °	1.917 to 33.183°	2.044 to 40.259	2.26 to 33.41
Limiting indices	$-8 \le h \le 6$, $-24 \le k \le 23$, $-36 \le l \le 36$	$-7 \le h \le 11$, $-27 \le k \le 27$, $-27 \le l \le 32$	$-14 \le h \le 14$, $-17 \le k \le 17$, $-19 \le l \le 19$	$-11 \le h \le 10$, $-14 \le k \le 14$, $-20 \le l \le 20$
Independent reflections	55783 R(int)=0.0295)	29446 (R(int)=0.0295)	31467 R(int)=0.0172)	12109 (R(int)=0.0268)
Absorption correction	multi-scan	multi-scan	multi-scan	multi-scan
Refinement method	Full-matrix least-squares on F^2	Full-matrix least-squares on F^2	Full-matrix least-squares on F^2	Full-matrix least-squares on F^2
Data/Restarints/Parameters	55783/0/192	29446/0/199	31467/0/208	12109/0/243
Goodness-of-fit on F^2	1.073	1.026	1.045	1.030
Final *R* indices [$I>2\sigma(I)$]	R1 = 0.0276, wR2= 0.0828	R1 = 0.0364, wR2= 0.0985	R1 = 0.0309, wR2= 0.0875	R1 = 0.0428, wR2= 0.1053
R indices (all data)	R1 = 0.0320, wR2 = 0.0864	R1 = 0.0489, wR2 = 0.0919	R1 = 0.0354, wR2 = 0.0909	R1 = 0.0624, wR2 = 0.1149

Table 2. Hydrogen bonds for compounds **1** and **3** [Å and °]

D–H···A	d(D–H)	d(H···A)	d(D···A)	<(DHA)
[8MAC-tsc)]				
O(1)…H(31)-N(3)	0.879	2.845	2.986	72.27
O(3)…H(32)-N(3)	0.854	2.217	3.061	169.82
N(3)-H(31)…O(1)	0.879	2.845	2.986	72.27
N(3)-H(32)…O(3)	0.854	2.217	3.061	169.82
Symmetry operation: **(x, y, z); : (-x, ½+y,1/2-z); (-x, -y, -z); (x, ½-y,1/2+z);**				
[8MAC-etsc)]				
O(1) …N(1)			3.034	
N(1) …O(1)			3.034	
Symmetry operation: **(x, y, z); (-x, -y, -z);**				

DNA binding studies

UV–Vis absorption spectral titrations

The electronic absorption spectra of compounds **1–4** (25 μM) in the absence and presence of CT-DNA (2.5–25 μM) are depicted in Fig. 7. The absorption bands of the compounds exhibited hypochromism of about 9.11, 13.89, 21.72 and 37.22 % with a blue shift of 2-5 nm at around 318-325 nm for compounds **1**, **2**, **3** and **4** respectively. In order to quantitatively determine the magnitude of the binding strength of the compounds with CT-DNA, the intrinsic binding constant K_{bin} was calculated from the ratio of slope to the y intercept in plots of [DNA]/[$\varepsilon_a-\varepsilon_f$] versus [DNA] (Fig. 8) and the values are found to be 2.2683±0.291 x10^5, 2.8738±0.372x10^5, 3.9088±0.310x10^5 and 1.2048±0.286x10^5. The obtained binding constant values, bathochromic shift and hypochromism showed that the compounds **1-4** behaved as potent binders to DNA through intercalation and the order of binding affinity of the complexes with CT-DNA is **3** > **2** > **1** > **4**. These results are comparable with earlier reports describing the intercalative mode of various intercalators [26,27].

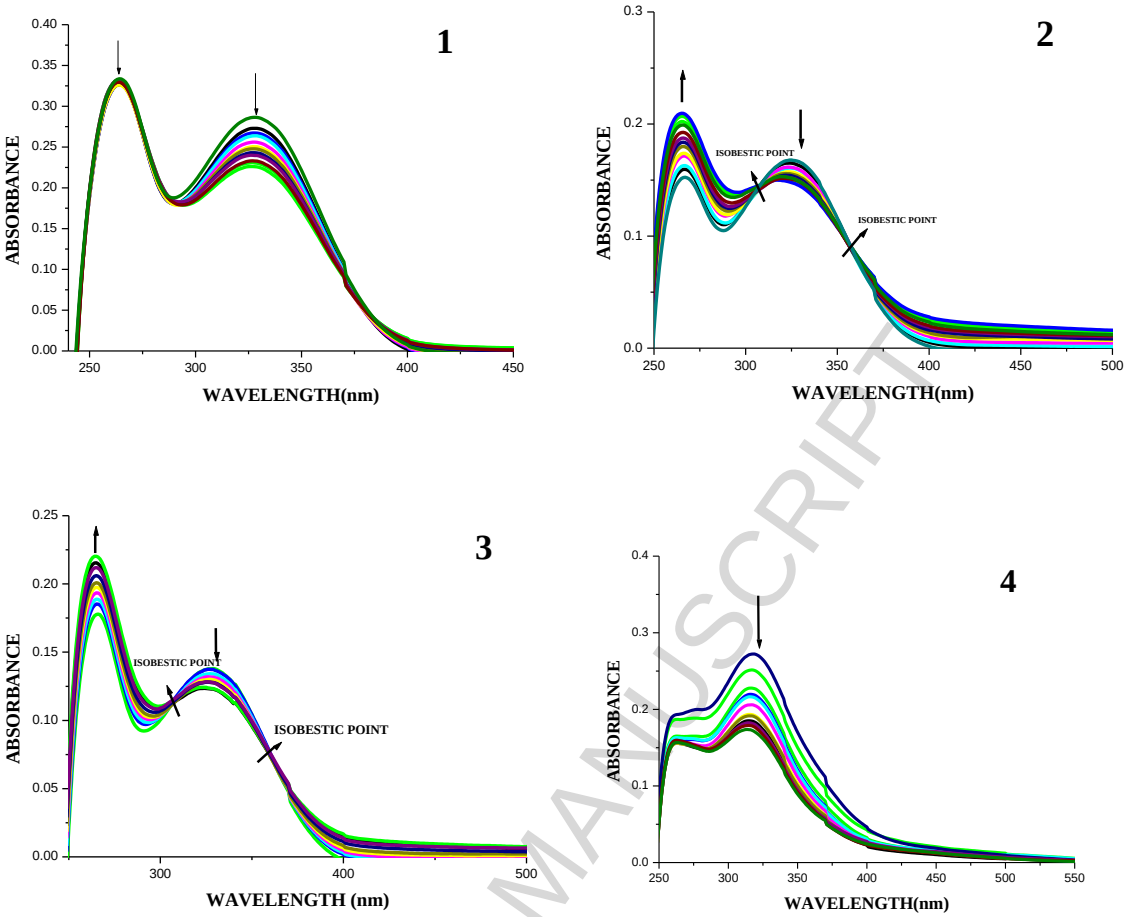

Fig.7. Absorption titration spectra of compounds (**1-4**) (25 µM) with increasing concentrations (2.5-25 µM) of CT-DNA (tris HCl buffer, pH 7.2)

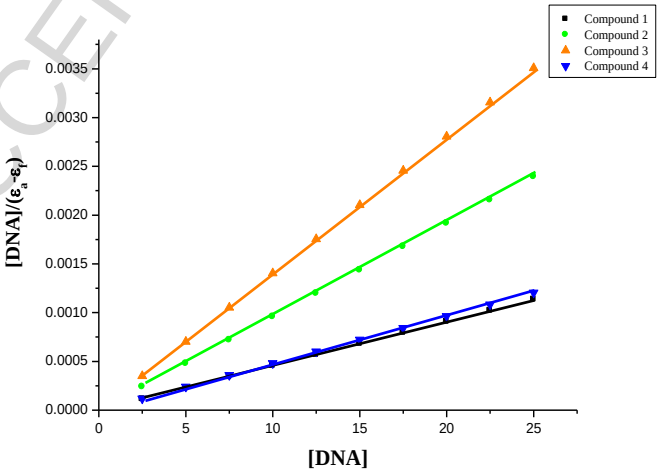

Fig. 8. Binding isotherms of the compounds **1-4** with CT-DNA

EB-DNA quenching studies

The competitive ethidium bromide displacement studies have been undertaken to gain deep insight into the interaction of the compounds with CT-DNA. The ability of a compound to affect the fluorescence intensity of an EB–DNA adduct is a reliable tool for the measurement of its affinity towards DNA. Relative binding of the compounds with EB-bound to CT-DNA is depicted in Fig. 9. On increasing the concentration of the compounds (10-100 µM) to CT-DNA pretreated with EB ([DNA]/[EB] = 1), quenching of the initial emission intensity was observed about 17.62, 19.16, 18.90 and 15.63 % together with a red shift of 2-3 nm for **1**, **2**, **3** and **4** respectively.

For a better quantitative understanding of the behavior of EB-DNA fluorescence suppression by coumarin Schiff bases, the magnitude of quenching was analyzed by the Stern-Volmer equation and the quenching constant determined by linear regression plot graph of (I_o/I) versus [Q] (Fig. 10) and the calculated quenching constant was found to be $3.24\pm0.009\times10^3$, $1.82\pm0.005\times10^3$, $2.05\pm0.004\times10^3$ and $5.77\pm0.002\times10^3$ for **1, 2, 3** and **4** respectively. The data showed that DNA-bound EB can be more readily replaced by the compounds and the obtained results concluded the intercalative mode of binding of the compounds with DNA.

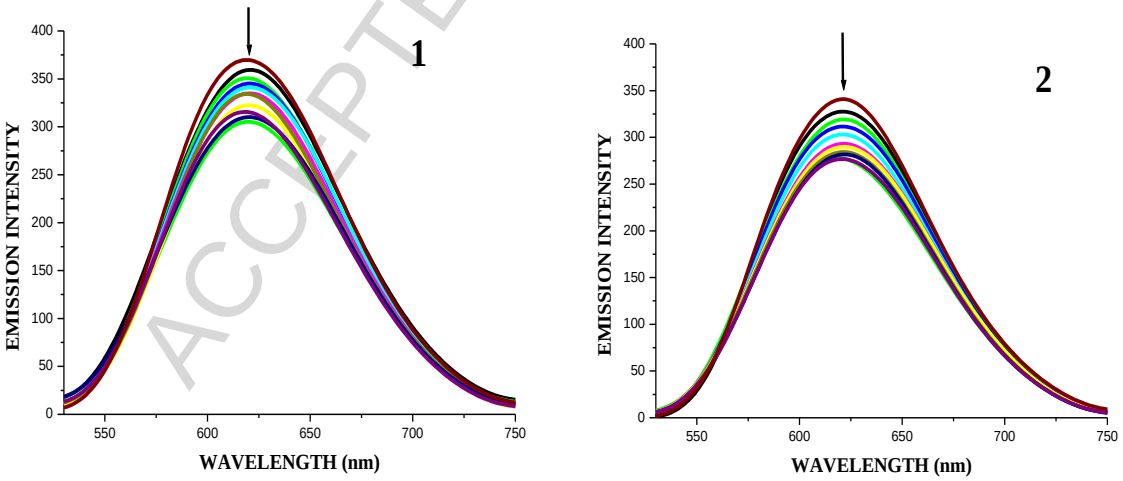

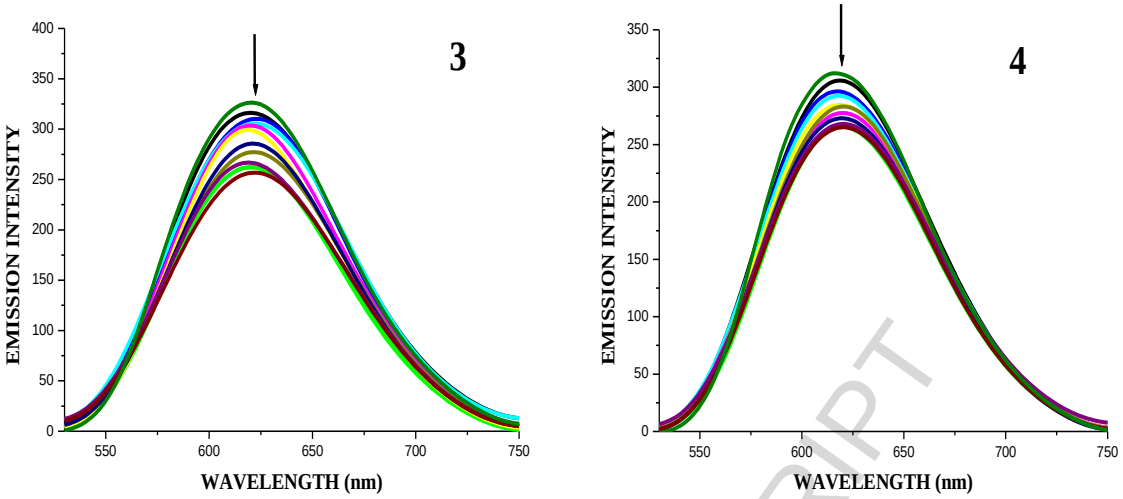

Fig. 9. The emission spectra of the DNA–EB system (λ_{exc}= 515 nm, λ_{em}= 530–750 nm), in the presence of compounds **1-4**. [DNA] = 10 µM, [compound] = 10–100 µM, [EB] = 10 µM. The arrow shows the emission intensity changes upon increasing compound concentration

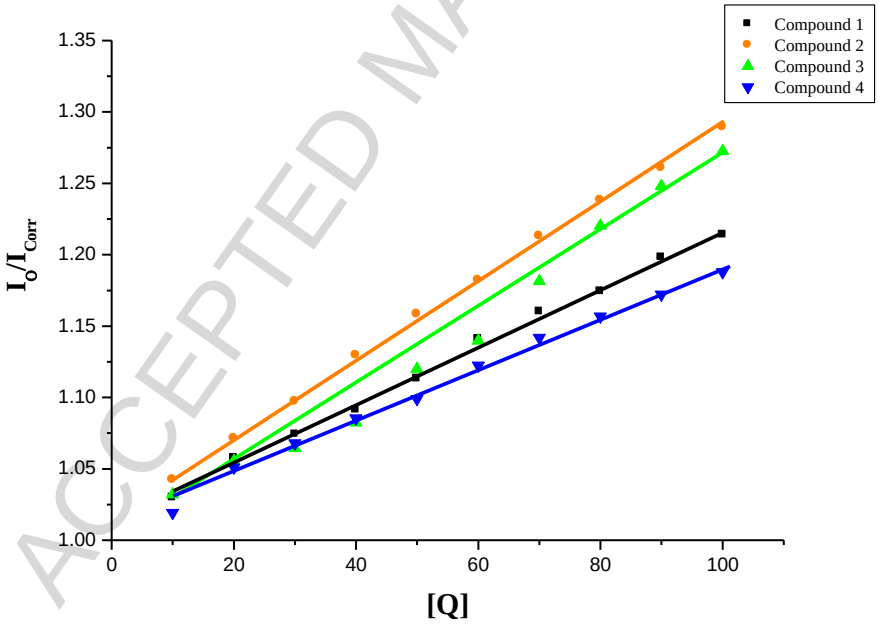

Fig. 10. Stern–Volmer plot of the fluorescence titration of compounds (**1-4**) (10-100 µM) with DNA-EB (10 µM)

Viscosity measurements

As a mean to investigate the binding mode of the compounds with DNA, viscosity measurements were carried out. A classical intercalation mode causes a significant increase in the viscosity of DNA solution due to an increase in the separation of base pairs at intercalation sites and hence an increase in overall DNA length [28,29]. As it is seen in Fig. 11, the viscosity of DNA (100 µM) increased slowly with increasing the concentration of compounds (20-100 µM) which showed that the coumarin Schiff bases bound to CT-DNA by intercalation mode which were encouraged by electron donating substitution on the *N*-terminal nitrogen of the compound and the increasing order of viscosity of CT-DNA by the compounds is **3** (NH-ethyl) > **2** (NH-methyl) > **1** (NH-hydrogen) > **4** (NH-phenyl).

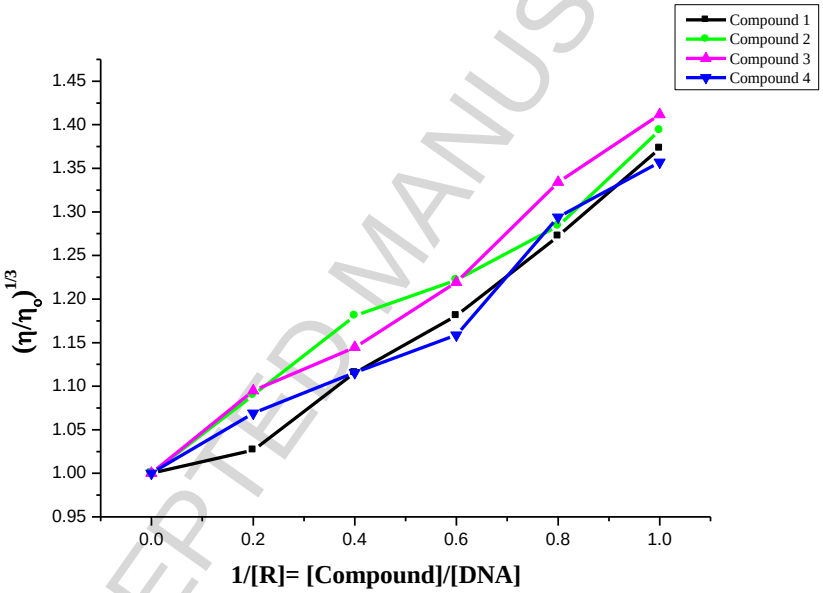

Fig. 11. Effect of the compounds (**1-4**) on viscosity of CT-DNA

Plasmid DNA pBR322 cleavage studies

Attempts were made to determine the chemical nuclease activities of the compounds by using supercoiled plasmid DNA pBR322 in Tris−acetic acid−ethylenediamine tetraacetic acid buffer pH 7.2 at 37 °C by 1.5 % agarose gel electrophoresis without any external agents. The cleavage efficiency was measured by determining the ability of the compound to convert the supercoiled DNA (SC Form) to linear circular form or nicked form (NC Form). All the compounds exhibited double-strand DNA cleavage to generate the LC form before

converting all of the SC form to NC form through single-strand break. From Fig. 12, we inferred that the compounds showed potent nuclease activity in the order of **3** > **2** > **1**≈ **4**, which may be due to the change in the electron accepting or donating ability pertaining to the *N*-terminal substituent of the compound. The observed result pattern is concise with their DNA binding affinity.

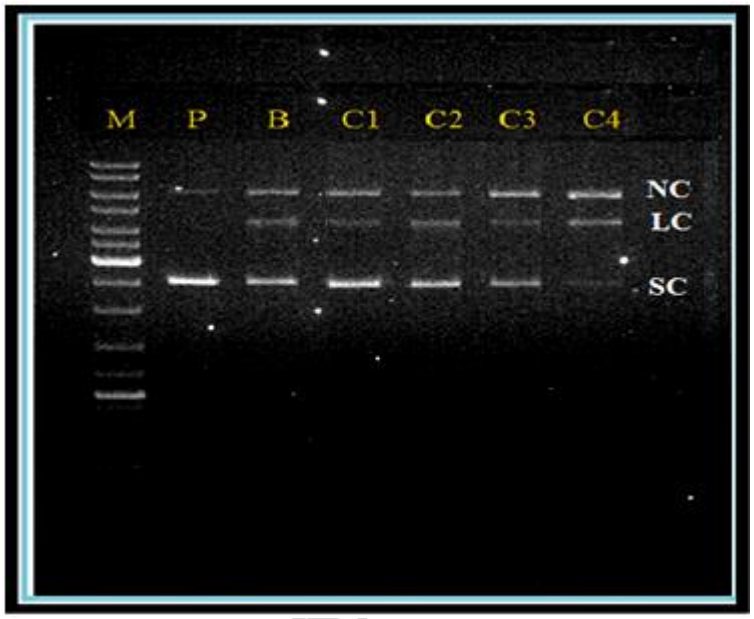

Fig. 12. Gel electrophoresis diagram showing the cleavage of supercoiled pBR322 DNA by compounds **1-4** in 5% DMSO and 95% 5 mM Tris−HCl/50 mM NaCl buffer at pH 7.2 and 37 °C with an incubation time of 2 h. Lanes M: Marker; Lane C1: compound 1 (50 μM). Lane C2: Compound 2 (50 μM); Lane C3: Compound 3 (50 μM); Lane C4: Compound 4 (50 μM. Forms SC, NC, and LC are supercoiled, nicked circular, and linear circular DNA, respectively.

Protein Binding Studies

The binding of compounds **1–4** with HSA and its homologue BSA was investigated by fluorescence emission spectroscopy, since the albumin solution exhibits an intense emission band (λ_{ex} = 290 nm) at $\lambda_{em,max}$ = 345 nm (for HSA) and 346 nm (for BSA) which is assigned to the existence of tryptophans. The emission titration studies have been performed at room temperature using BSA (10 μM)/ HSA (10 μM) with increasing concentrations of compounds **1–4** (0−100 μM) in the range 290−500 nm (Fig. 13-14). Addition of the above test compounds to BSA solution resulted in a significant decrease in the fluorescence intensity of BSA at 346 nm, up to 62.65, 44.51, 74.87 and 49.84 % of the initial fluorescence intensity of

BSA with blue shift of 2-5 nm for **1**, **2**, **3** and **4** respectively. Addition of the compounds to HSA solution resulted in a quenching of the emission band of HSA at 345 nm up to 48.89, 36.03, 47.13, 40.55 of the initial fluorescence intensity together with a blue shift of 2-4 nm for **1**, **2**, **3** and **4** respectively (Fig. 13-14). From the above observations, we may conclude that definite interaction is taking place between the compounds and serum albumins.

The absorption spectra of BSA/HSA in the absence and presence of compounds are given in Fig. S7. In the presence of compounds **1-4**, the absorbtion intensity of BSA/HSA exhibited hypochromism with a 2-3 nm of hypsochromic shift, indicating a static quenching mechanism of the serum albumins by the compounds.

By using Stern Volmer quenching equation, the values of the Stern Volmer quenching constant (K_{SV}) and the quenching constant (K_q) for compounds interacting with serum albumins (BSA or HSA) were calculated [30]. The Stern Volmer quenching constant results follows the order **3** > **2** > **1** > **4** and the observed Ksv values are comparable to those reported for thiosemicarbazone compounds [27]. The quenching constant values for the quenching of the serum albumins by the compounds ($k_q \approx 10^{12}$ M^{-1} s^{-1}) suggested the good binding affinity of the compounds with serum albumins through static quenching mechanism [30]. The binding constant K_{bin} and number of binding site (n) can be calculated from the Scatchard equation and are given in Table 3 (Fig. 16), from these values we knew that the compounds **1-4** showed strong binding affinity with serum albumins. The obtained binding constant and quenching constant values revealed that the compounds bind to both the albumins in the following order **3** > **2** > **1** > **4** and the results are consistent with the trend followed by them in their DNA binding profile. This observed fashion can be explained on the basis of hydrophobicity of the compounds. As seen from the results, complex **3** with the enhanced hydrophobicity showed the best binding ability [31]. The obtained quenching constant and binding constant values of these coumarin Schiff bases agree well with those reported for Schiff bases [26,27].

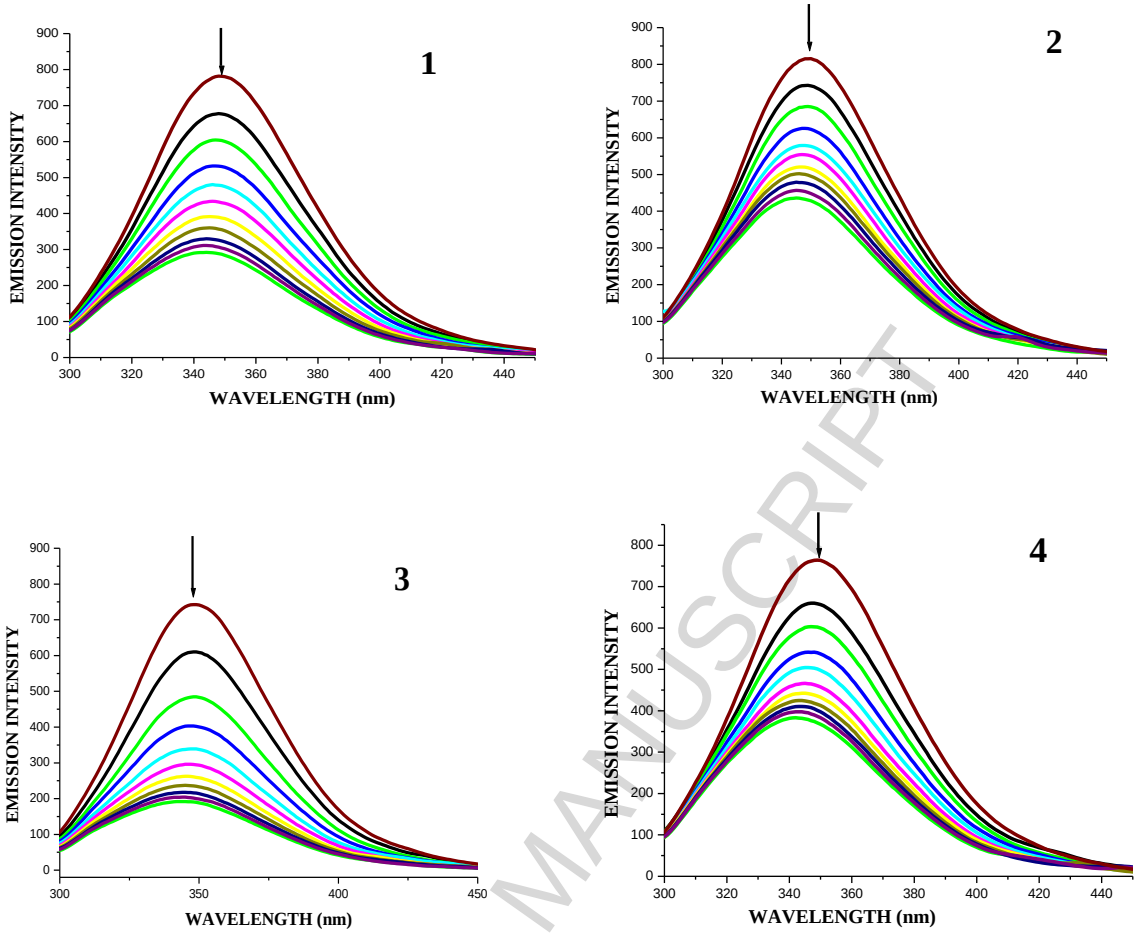

Fig. 13. The emission spectra of BSA (10 μM; λ_{exc}= 280 nm; λ_{emi}= 346 nm) in the presence of increasing amounts of compounds **1-4** (10–100 μM). The arrow shows the emission intensity changes upon increasing compound concentration

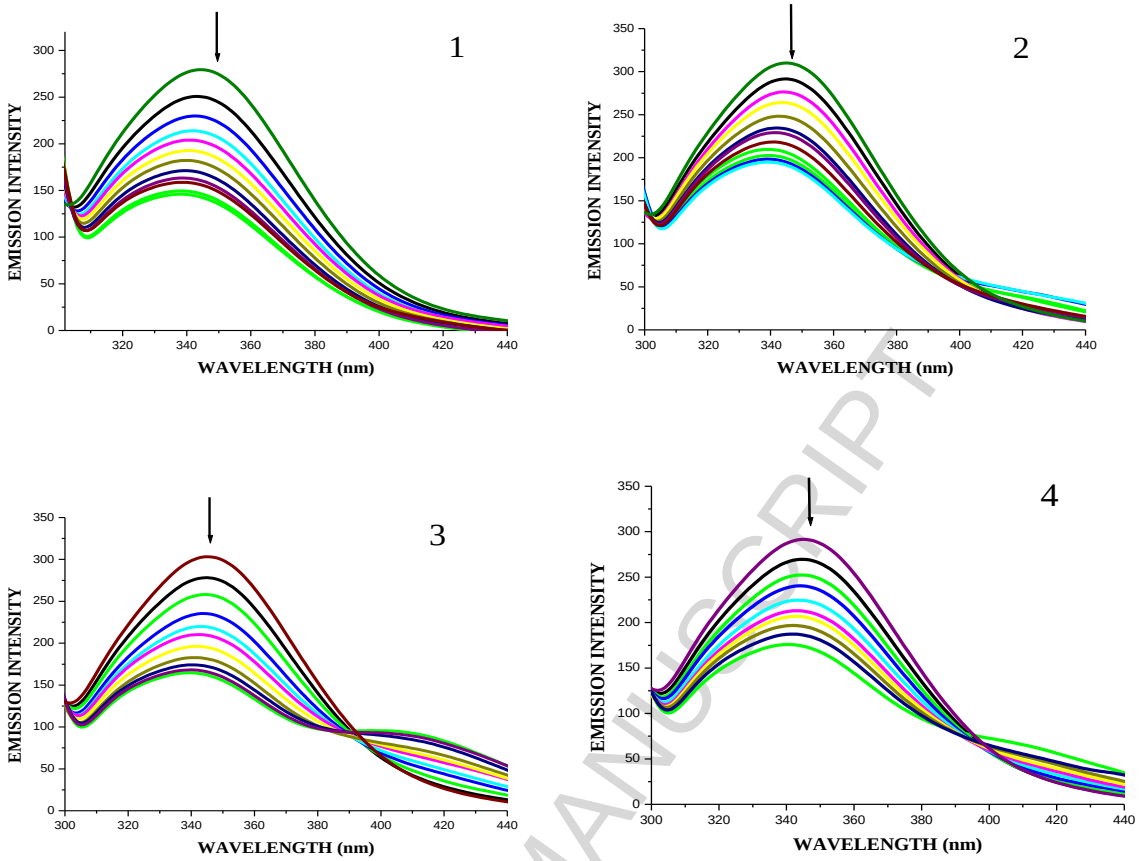

Fig. 14. The emission spectra of HSA (10 μM; λ_{exc}= 280 nm; λ_{emi}= 346 nm) in the presence of increasing amounts of compounds **1-4** (10–100 μM). The arrow shows the emission intensity changes upon increasing compound concentration

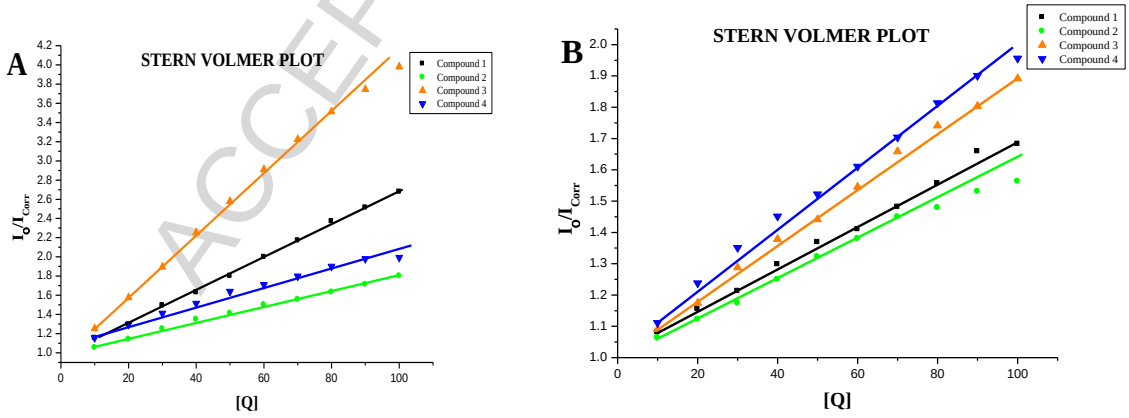

Fig. 15. **A**) Stern–Volmer plot of the fluorescence titration of the compounds (**1-4**) (10-100 μM) with BSA (10 μM). **B**) Stern–Volmer plot of the fluorescence titration of the compounds (**1-4**) (10-100 μM) with HSA (10 μM)

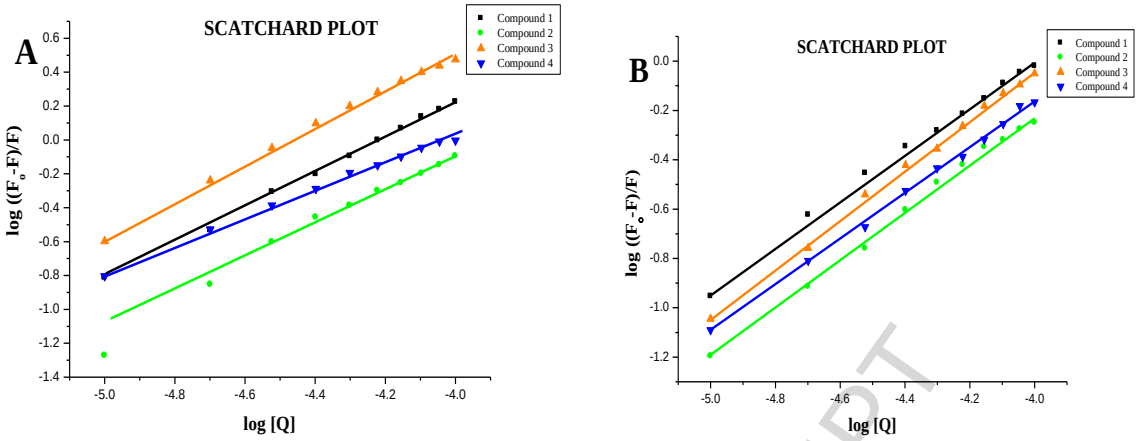

Fig. 16. **A**) Scatchard plot of the fluorescence titration of the compounds (**1-4**) (10-100 µM) with BSA (10 µM). **B**) Scatchard plot of the fluorescence titration of the compounds (**1-4**) (10-100 µM) with HSA (10 µM)

Table 3. Stern Volmer quenching constant (K_{sv}), Quenching constant (k_q), binding constant (K_{bin}) and number of binding sites (n) for the interactions of compounds 1-4 with BSA/HSA

Compounds	Stern-Volmer quenching constant K_{sv}/M^{-1}	Quenching Constant (k_q) $M^{-1}s^{-1}$	Binding constant K_{bin}/M^{-1}	n
BSA				
1	$1.724\pm0.032\times10^{4}$	$1.724\pm0.032\times10^{12}$	$2.790\pm0.059\times10^{4}$	1.0543±0.013
2	$0.890\pm0.019\times10^{4}$	$0.890\pm0.019\times10^{12}$	$3.195\pm0.019\times10^{4}$	1.0421±0.045
3	$3.095\pm0.016\times10^{4}$	$3.095\pm0.016\times10^{12}$	$6.514\pm0.091\times10^{4}$	1.007±0.020
4	$0.950\pm0.039\times10^{4}$	$0.950\pm0.039\times10^{12}$	$1.884\pm0.086\times10^{3}$	0.8198±0.019
HSA				
1	$0.933\pm0.020\times10^{4}$	$0.933\pm0.020\times10^{12}$	$4.661\pm0.020\times10^{3}$	0.9177±0.021
2	$0.578\pm0.018\times10^{4}$	$0.578\pm0.018\times10^{12}$	$4.927\pm0.020\times10^{3}$	0.9784±0.021
3	$0.898\pm0.014\times10^{4}$	$0.898\pm0.014\times10^{12}$	$9.395\pm0.014\times10^{3}$	1.0030±0.015
4	$0.681\pm0.014\times10^{3}$	$0.681\pm0.014\times10^{12}$	$3.692\pm0.014\times10^{3}$	0.9326±0.015

Conformational Investigation

In the synchronous fluorescence spectra of the tyrosine residue of both the serum albumins, the addition of the compounds to the serum albumin solution showed hypochromism with negligible shift in the emission wavelength (Fig. S8-S9). Synchronous fluorescence spectra at $\Delta\lambda$ = 60 nm of BSA and HSA solution exhibited a decrease in fluorescence intensity up to 43.23-50.00 % and 36.20-49.54 % at 340 nm with significant blue shift for compounds **1-4** respectively (Fig. S10-S11). The obtained results showed that the test compounds effectively affect the microenvironment of the tryptophan and tyrosine micro regions.

Three-dimensional fluorescence spectra analysis

To further study the nature of microenvironmental changes occurring in serum albumins during interaction with the compounds, 3D fluorescence spectroscopic studies have been carried out. Fig. 17-18 shows the changes encountered in 3D emission spectra of serum albumins in the absence and presence of compounds and their corresponding characteristic parameters are given in Table S2. On adding the compounds to serum albumins, the fluorescence intensity of Rayleigh first order scattering peak increased, which is due to the compound formation of serum albumins with our compounds leading to an increase in the diameter of the macromolecule which in turn resulted in the enhancement of scattering effect [32]. The emission intensity of peak 'B' corresponding to the tryptophan and tyrosine residues decreased with slight blue shift. The obtained results revealed that conformational changes and the molecular micro-environment of serum albumins occurred after interaction with the compounds.

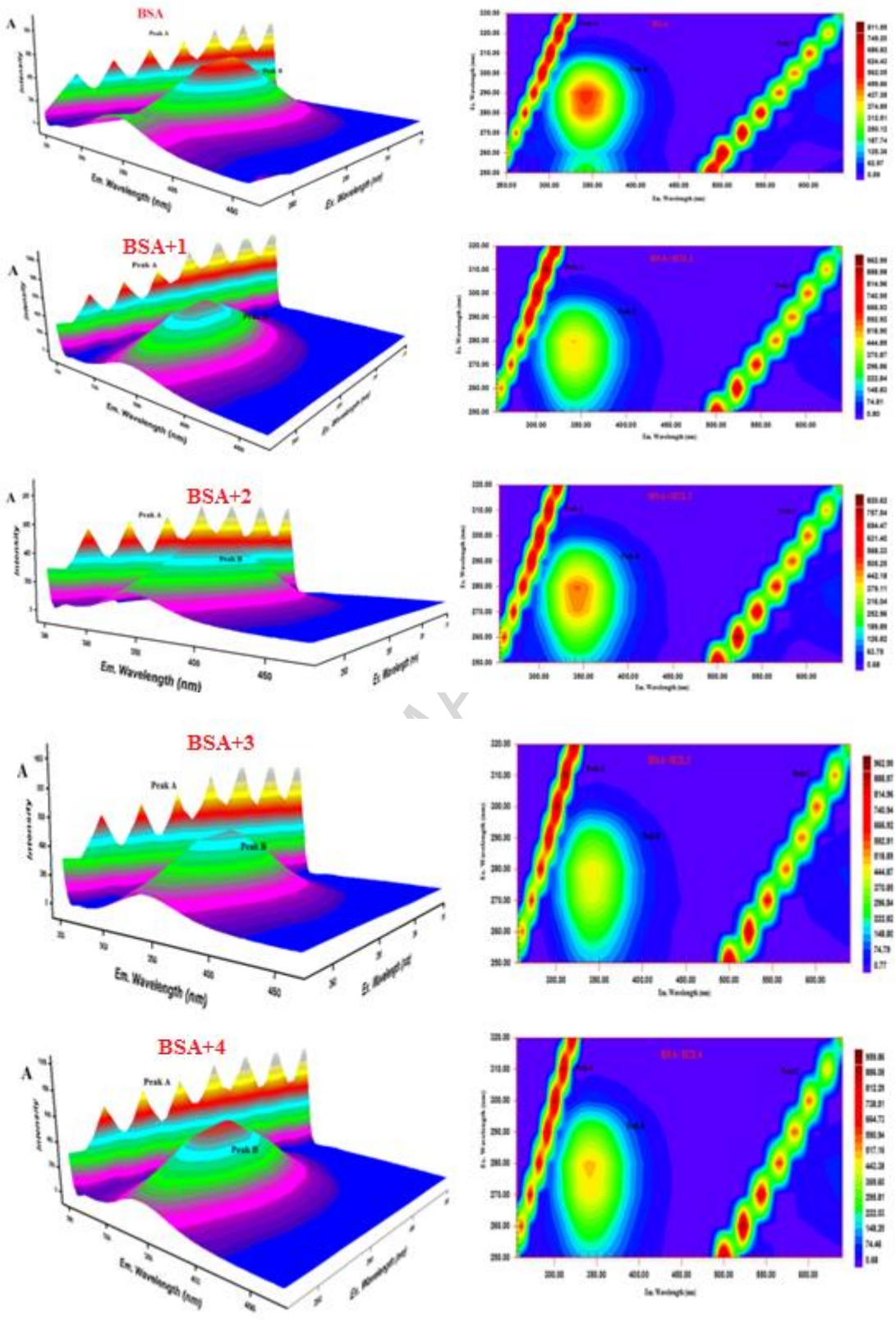

Fig. 17. Three-dimensional fluorescence spectra of BSA in the absence and presence of compounds (**1-4**) (pH 7.4, 298 K, [BSA] =10 μM, [Compound] =10 μM)

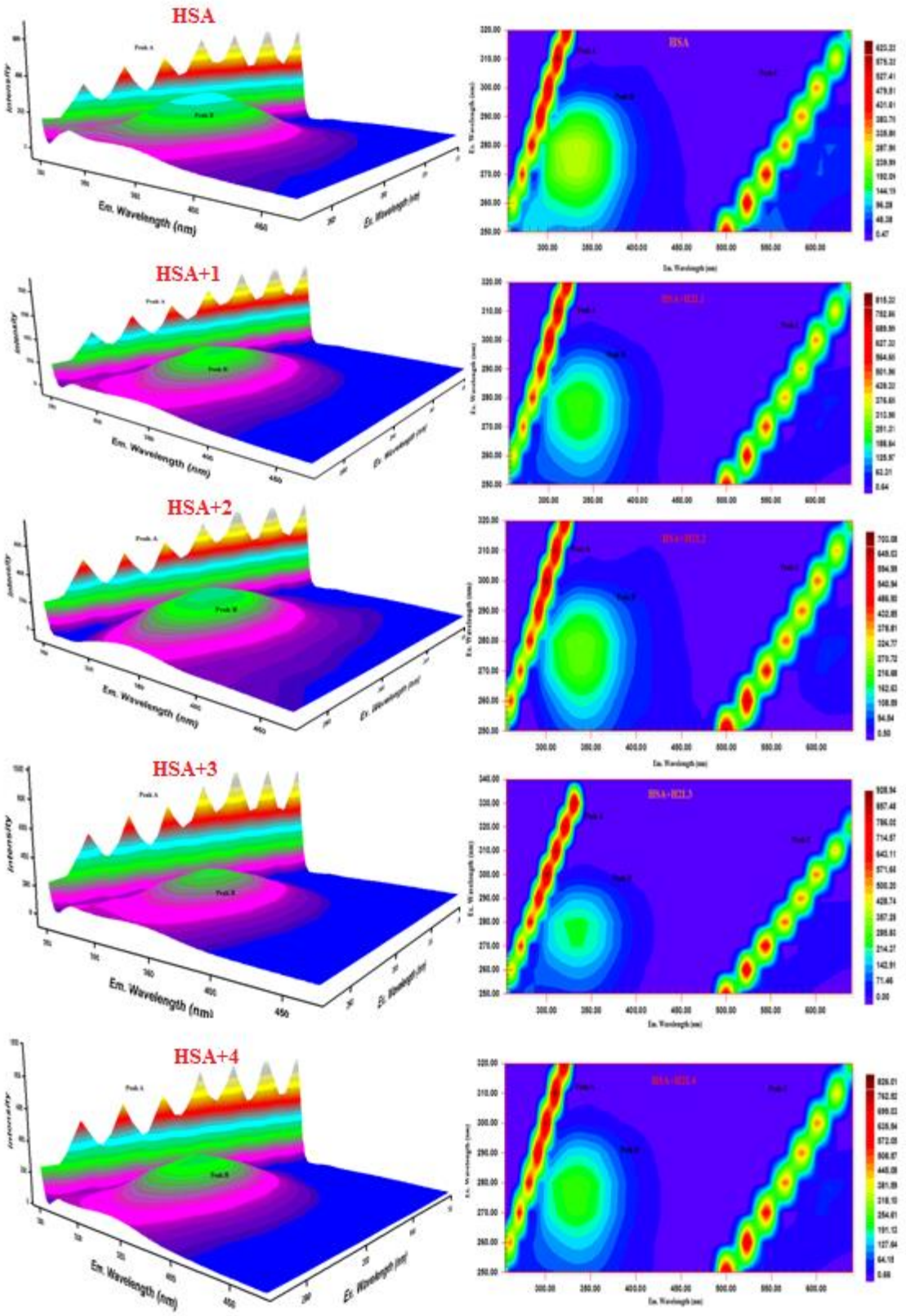

Fig. 18. Three-dimensional fluorescence spectra of HSA in the absence and presence of compounds (**1-4**) (pH 7.4, 298 K, [HSA] =10 μM, [compound] =10 μM)

In vitro Antioxidant activity

The compounds which exhibit radical scavenging activity are receiving much attention because they possess interesting anticancer, anti-ageing and anti-inflammatory activities [33]. The analysis of the DPPH radical scavenging ability of 3-acetyl-8-methoxy-coumarin-4(*N*)-substituted thiosemicarbazones have been carried out along with the standard Vitamin C. The results showed that the activity of the compounds (68.45-92.67 µM) is higher than that of the standard 98.72±1.50 µM (Fig. 19; Table 4), in which compound **3** shows the best DPPH scavenging activity. In phosphomolybdenum assay, the antioxidant capacity is expressed as the number of equivalents of ascorbic acid (Table 5). A comparison of the radical scavenging activity of compounds **1–4** with that of the reported Schiff base compounds may reveal that coumarin appended thiosemicarbazones **1–4** act as potent radical scavengers [22,34,35].

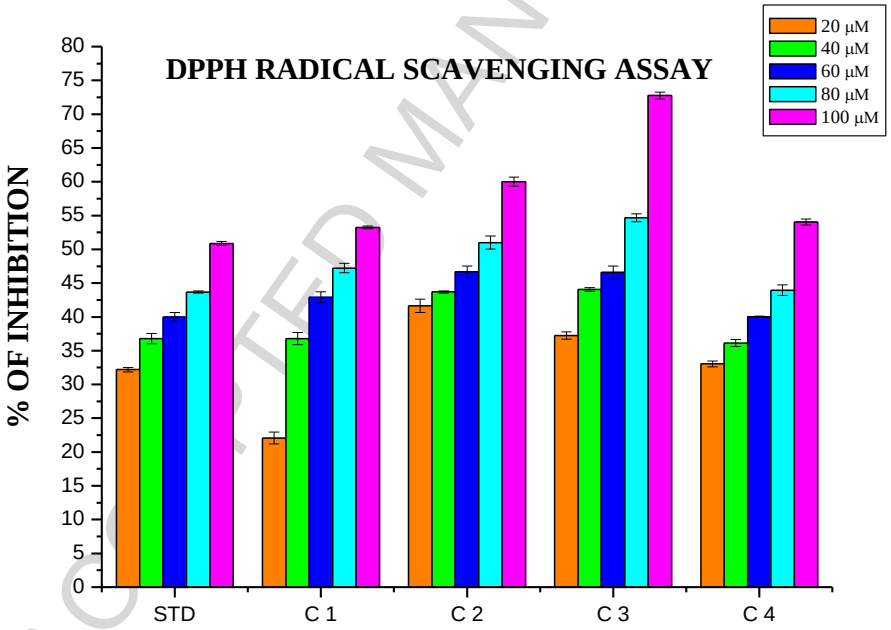

Fig. 19. DPPH scavenging activity of compounds (**1-4**). Error bars represent the standard deviation of the mean (n=3)

Table 4. The DPPH radical scavenging activity of the compounds **1-4**

COMPOUNDS	IC_{50} VALUE (µM)
Ascorbic acid	98.72±1.50
1	89.79±1.23
2	77.23±0.93
3	68.45±0.87
4	92.67±1.60

Table 5. Estimation of Total antioxidant capacity of compounds **1-4**

Compounds	µg Ascorbic acid equivalents/ml
1	37.74±0.57
2	39.12±0.68
3	43.53±0.74
4	34.42±0.39

Antimicrobial activity

In vitro antimicrobial activities of the compounds **1–4** were examined with few fungi *A. niger*, *A. fumigatus C. albicans*, *C. tropicalis* and *T. rubrumi* and some pathogenic bacteria such as *S. aureus*, *S. paratyphi*, *P. aeruginosa* and *S. pneumonie*, and the results are expressed as the zone of inhibition and minimum inhibitory concentration (MIC) (Fig. 20-21; Table S3-S6). *Ketaconazole* and *Gentamicin* were used as the positive controls for fungi and bacteria respectively and their MIC values are also given for comparison purpose. The control disc with negative control (10 % aqueous DMSO) exhibited no zone of inhibition. From the zone of inhibition values, we knew that antimicrobial activity of the compounds was increased while increasing the concentration of the compounds. In antibacterial studies, compounds **3** and **4** showed similar minimum inhibitory concentrations on *S. aureus* followed by **2** and **1.** Compound **4** was more active on *P. aeruginosa*, *S. pneumonie* and *S. paratyphi* and the activity of the compounds in the order of **4** > **3** > **2** > **1**. 4(*N*)-phenyl substituted coumarin thiosemicarbazones stood out as the best when employed against the five different fungal species and the activity follows the order of **4** > **3** > **2** > **1**. When tested against *C. albicans* complex **4** stood out as good followed by the complexes **2, 3** and **1** respectively. Due to the structural variations of compounds and variation on the group of microorganisms, the compounds (**1-4**) exhibited different degree of activity [36]. The activities of these

compounds were comparable to the thiazolyl coumarin derivatives reported by Hasnah *et al* [37,38] and some other reported Schiff bases, showing that our compounds showed significant activity [27,35,37-41].

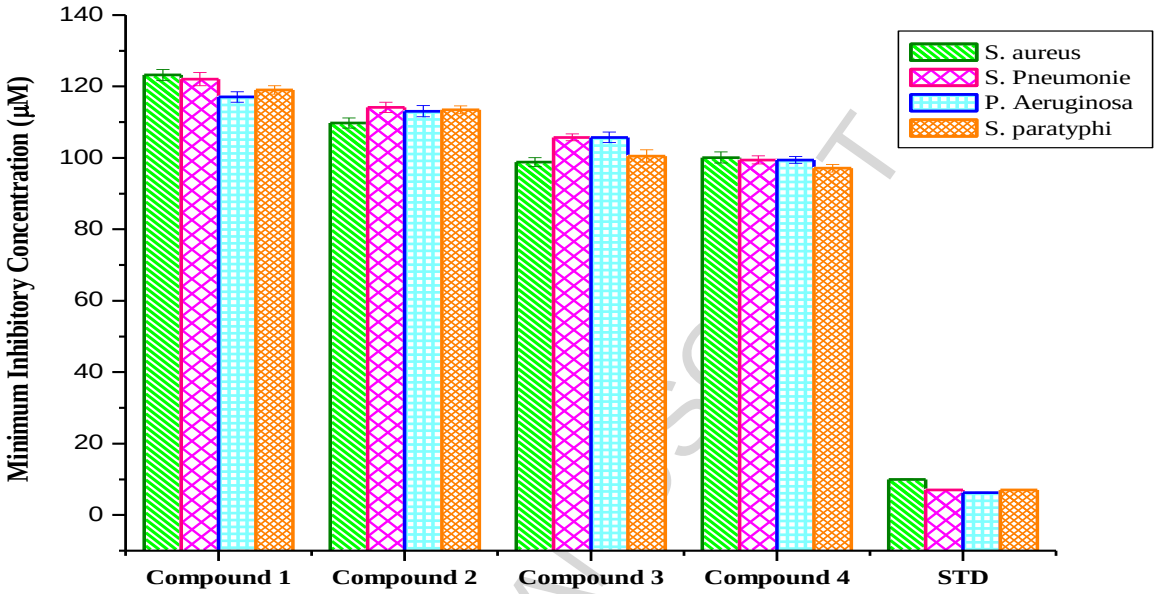

Fig 20. Anti bacterial activity of compounds (**1-4**). Error bars represent the standard deviation of the mean (n=3)

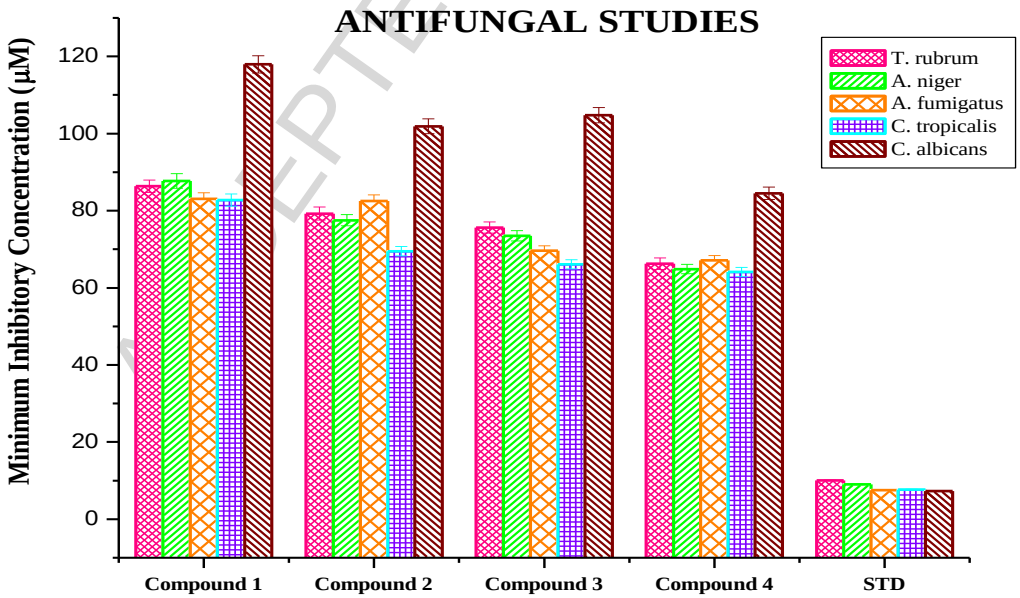

Fig. 21. Anti fungal activity of compounds (**1-4**). Error bars represent the standard deviation of the mean (n=3)

Cytotoxicity studies

Antiproliferative Studies - Cancer Cell Growth Inhibition

Our synthesized compounds act as potent DNA/Protein binders and free radical scavengers, which prompted us to evaluate the possible antiproliferative effects of the 3-acetyl-8-methoxy-coumarin appended Schiff bases **1-4** with the breast cancer cells (MCF-7) and lung cancer cell lines (A549) using MTT assays. The dose dependent cell death inducing ability of the compounds has been investigated by using the percentage of cell viability versus compound concentration plot (Fig. 22-23), which showed that our compounds differentially inhibit the tumor cell viability, depending on the dose applied. On increasing the concentration, our compounds **1-4** exhibited a higher decrease in the cell viability. The results were analyzed by means of cell inhibition expressed as IC_{50} values and are given in Table 6. As shown in Table 6, IC_{50} values for the test compounds ranged from 11.31 µM to 12.65 µM with both the cell lines. The results showed that the compounds **1-4** exhibited significant cytotoxic activities than the standard drug *cisplatin* against the MCF-7 and A549 cells. The antiproliferative activity of the compounds follows the order *cisplatin* (16.79±0.08) < **4** (12.19±0.20) ≈ **1** (12.15±0.23) < **2** (11.77±0.29) < **3** (11.31±0.15) in human breast cancer cell lines (MCF-7). In human lung cancer cells (A549), the compounds exhibited anticancer activity in the order of *cisplatin* (15.10±0.05) < **4** (12.65±0.16) < **1** (12.48±0.14) < **2** (11.98±0.19) < **3** (11.46±0.14).

Electron withdrawing phenyl substituent at terminal nitrogen possesses somewhat poor inhibitory activity compared to other compounds (**1-3**), which is in agreement with its lower binding propensity towards DNA. Alkyl substituted at terminal nitrogen atom containing compounds showed improved anticancer activity. On the basis of results, the anticancer activity of the compounds has been arranged in the order **3** > **2** > **1** > **4**. To investigate the selectivity of the compounds for cancer cells rather than normal cell lines, compounds were screened for their activity on the human normal keratinocyte cells (HaCaT), the results confirmed the non-toxic nature of the compounds. Cytotoxic nature of our compounds are superior to those reported Schiff base compounds against MCF-7 cells and A549 cells [27,42,43].

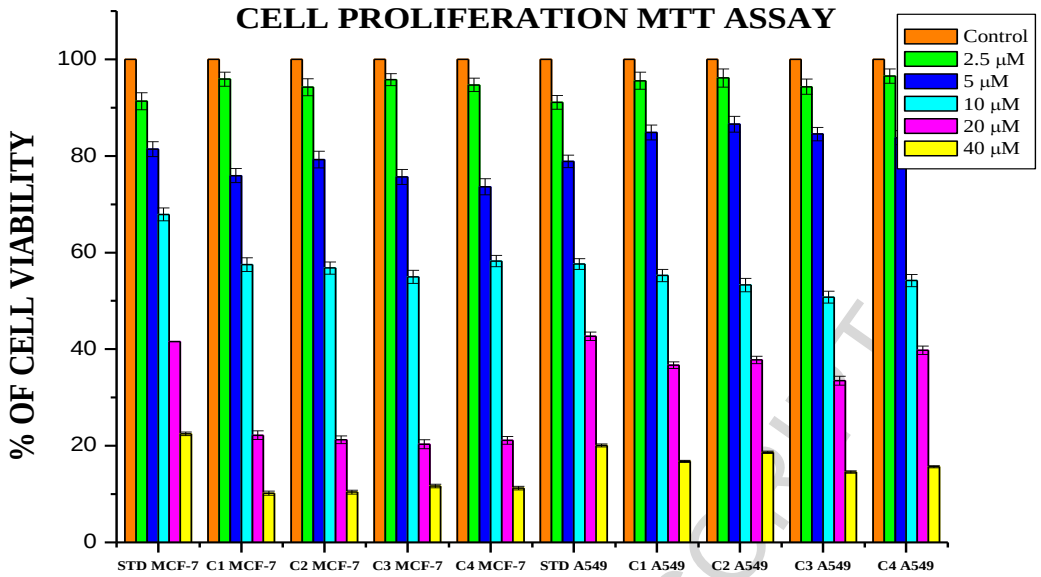

Fig. 22. The compounds **1-4** and *Cisplatin* inhibit MCF-7 and A549 cells proliferation in a dose dependent manner. MCF-7 and A549 cells were treated with different concentrations of compounds for 48 h, the cell viability was determined and the results were expressed as percentage cell viability with control. Results shown are mean, which are three separate experiments performed in triplicate

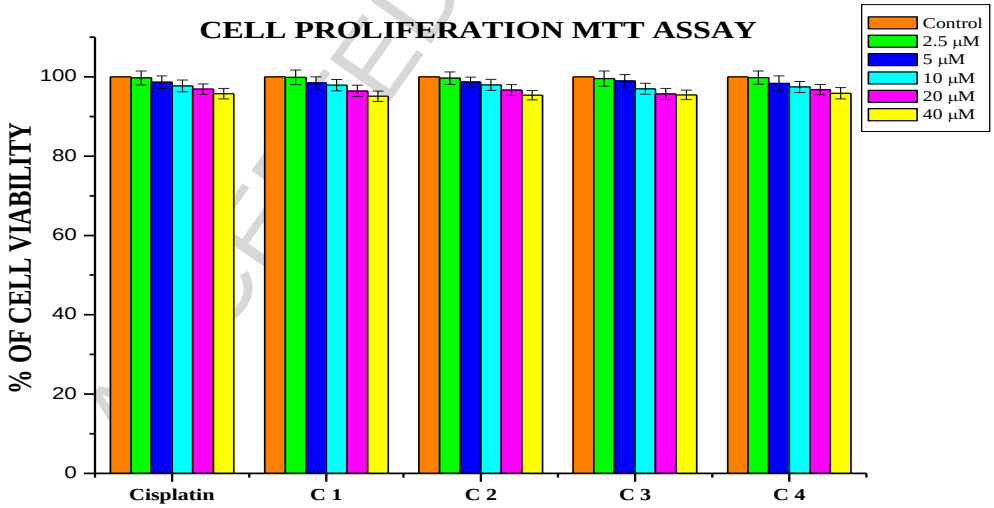

Fig. 23. The newly compounds **1-4** and *Cisplatin* inhibit HaCaT cells proliferation in a dose dependent manner. HaCaT cells were treated with different concentrations of compounds for 48 h, the cell viability was determined and the results were expressed as percentage cell viability with control. Results shown are mean, which are three separate experiments performed in triplicate.

Table 6. The IC_{50} values for the human breast cancer cell line MCF-7, human lung carcinoma cancer cell line A549 and human normal keratinocyte cells (HaCaT) with the compounds **1-4** for 48h

Compounds	IC_{50} values (μM)		
	MCF-7	A549	HaCaT
Cisplatin	16.79±0.08	15.10±0.05	>40
1	12.15±0.23	12.48±0.14	>40
2	11.77±0.29	11.98±0.19	>40
3	11.31±0.15	11.46±0.14	>40
4	12.19±0.20	12.65 ±0.16	>40

LDH assay

LDH assay act as an indicator of cell membrane integrity. It is a stable cytoplasmic enzyme, which released into the culture medium due to the loss of membrane integrity resulting from apoptosis of cells. To further investigate the drug induced cytotoxicity of cancer cells [44], LDH assay have been carried out with cancer cell lines such as A549 and MCF-7. These cancer cells were treated with the IC_{50} concentration of the compounds **1-4** for a period of 48 h, a considerable increase in the level of LDH released into the culture medium was observed (Fig. 24). The compounds showed good level of LDH leakage in A549 and MCF-7 cells compared to *cisplatin*. These results authenticated that the effectiveness of the compounds in inducing cell death by collapsing the membrane integrity. The order of increased induction of LDH release by the compounds was found to be **3** > **2** > **1** > **4**. The coumarin appended thiosemicarbazones showed potent activity when compared with the earlier reports [45].

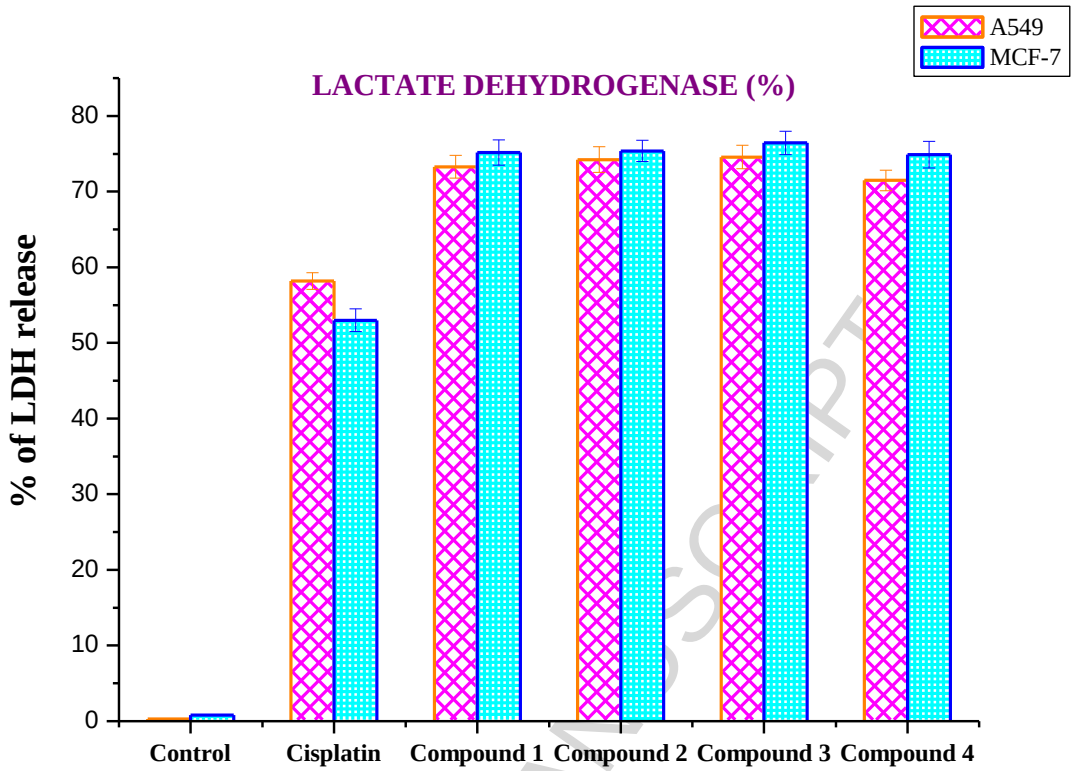

Fig. 24. Percentage of lactate dehydrogenase released by the human cancer cell lines A549 and MCF-7 after an incubation period of 48 h with compounds **1-4**. Error bars represent the standard mean error (n= 6).

Nitric oxide assay

A well-known short-lived free radical Nitric oxide produced non-enzymatically by NOS, causes damage in most of the biomolecules, including protein and DNA. Nitric oxide has been shown to directly inhibit methionine adenosyl transferase, leading to glutathione depletion and its reaction with superoxide generates the strong oxidant peroxynitrite, which can initiate lipid peroxidation or cause a direct inhibition of the mitochondrial respiratory chain [46]. In the present study NO release by the compounds **1-4** was evaluated using A549 and MCF-7 cells. From the results, it is concluded that the compounds were found to release more NO than the control and *cisplatin* (Fig. 25), in which compound **3** was more potent in increasing the level of NO in the culture medium followed by **2**, **1** and **4.** The results of the present study revealed the significant anticancer potential of the compounds (**1–4**) and our results are significant when compare to the reported results [45].

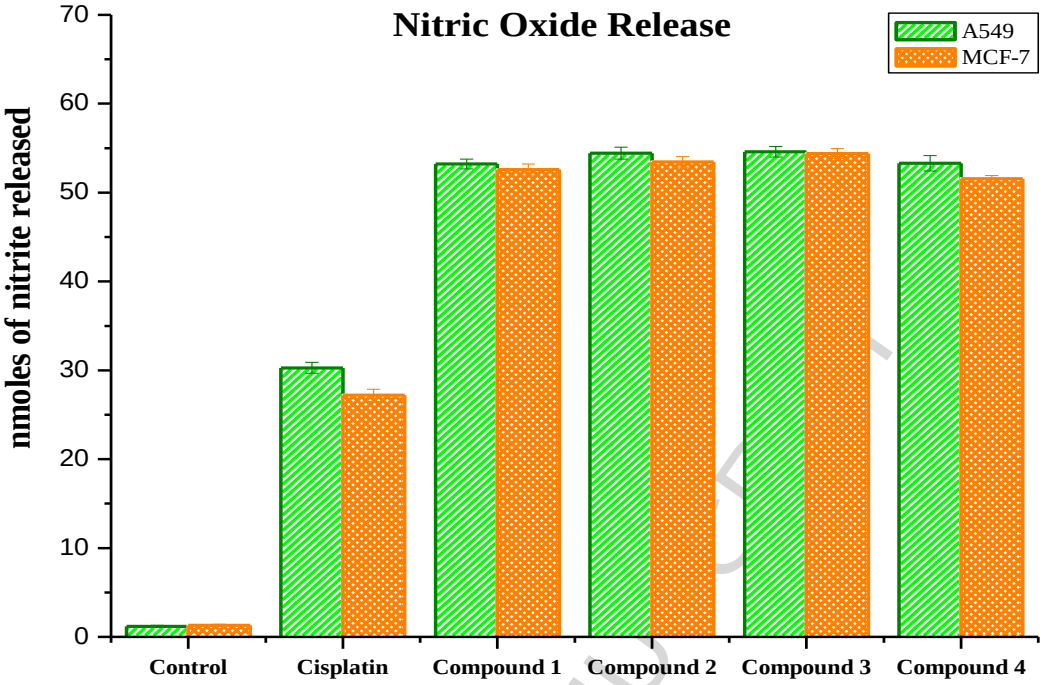

Fig. 25. Nitrite released (nmoles) by the human cancer cell lines A549 and MCF-7 after an incubation period of 48 h with compounds **1-4**. Error bars represent the standard mean error (n= 6).

Conclusion

Four coumarin appended thiosemicarbazone derivatives (**1-4**) were synthesized and characterized by using analytical and spectral techniques. The respective crystal structures were resolved by means of X-ray diffraction studies. The compounds intercalatively bound to CT-DNA, as supported by EB displacement studies and viscosity measurements. Protein binding studies indicated that the quenching mechanism is static and the micro environmental changes occurred has been confirmed by 3D fluorescence experiment. Similar to the reported coumarin derivatives, the compounds were able to scavenge the free radicals and inhibit the growth of all the tested bacterial and fungal pathogens. The outcome from the MTT assay revealed the anticancer potential of the compounds, with an activity greater than *cisplatin*. Combining the overall results, it is evident that the biological activity of the compounds follows the pattern **3** > **2** > **1** > **4** and the promising results obtained from the biological studies suggested that the compounds can act as good probes for further exposure in pharmaceutical applications.

Experimental section

Materials

Analar or chemically pure grade reagents were used and solvents were purified/dried according to standard procedures [47]. The compounds such as 3-Acetyl-8-methoxycoumarin-4(*N*)-substituted thiosemicarbazones were prepared with a slight modification of the literature procedures [23,37,38,48]. The techniques used for the characterization of the compounds are given in supporting information.

Preparation of 3-acetyl-8-methoxy-2H-chromen-2-one [37]

3-Acetyl-8-methoxycoumarin was prepared from 3-methoxysalicylaldehyde (1.22 g, 1 mmol) and ethylacetoacetate (1.95 g, mmol) in the presence of catalytic amount of piperidine as described in standard literature methods [37]. Yield = 95 %. Mp. 123 °C; UV-Vis (DMSO), λ_{max} (ε): 316 (21,770) nm ($dm^3mol^{-1}cm^{-1}$); IR (ν, cm^{-1}): ν(C=O lactone) 1731, ν(C=O acetyl group) 1683. ^{1}H NMR (400 MHz, DMSO-d_6, δ ppm, J Hz): δ 8.62-8.62 (d, *J*=1.6, 1H, C3-H), δ 7.47-7.49 (dd, J= 0.8, 6.6, 1H, C5-H), δ 7.31-7.35 (m, 1H, C6-H), δ 7.41-7.43 (dd, J= 0.8, 6.2, 1H, C7-H), δ 3.91 (s, 3H, -OCH_3), δ 2.57 (s, 3H,-CH_3).

Synthesis of ((1*E*)-1-(1-(8-methoxy-2-oxo-2H-chromen-3yl)ethylidene) thiosemicarbazide) [8MAC-tsc] (1) [37]

3-acetyl-8-methoxy-2H-chromen-2-one (1 g, 4.58 mmol) was dissolved in 20 cm^3 methanol. To this, methanolic solution (30 cm^3) of thiosemicarbazide (0.417 g, 4.58 mmol) was added and to this, catalytic amount of glacial acetic acid was added and the mixture was refluxed for 2 h with continuous stirring. A yellow compound precipitated was collected by filtration, washed well with cold methanol and dried under vacuum. The compound was recrystallized from DMF-Methanol (1:9 v/v) to yield yellow single crystals suitable for X-ray analysis. Yield: 76 %. M.p: 201 °C. FT-IR (ν, cm^{-1}) in KBr: ν(C=O lactone) 1713, ν(C=N) 1612, ν(-NH_2) 3344, ν(-NH) 3187, ν(C=S) 770. UV-Vis (DMSO), λ_{max} (ε): 335 (14,472) nm ($dm^3mol^{-1}cm^{-1}$). ^{1}H NMR (400 MHz, DMSO-d_6, δ ppm, J Hz): δ 7.95 (s, 1H, C4-H), δ 7.28-7.32 (m, 3H, Ar-H), δ 3.90 (s, 3H,-OCH_3), δ 2.23 (s, 3H,-CH_3), δ 10.43 (s, 1H, NH-C=S), δ 8.39 & 8.44 (2s, 2H, -NH_2).

The very similar method was used to prepare the following compounds.

Synthesis of ((1*E*)-1-(1-(8-methoxy-2-oxo-2H-chromen-3-yl)ethylidene)-4(*N*)-methyl thiosemicarbazide) [8MAC-mtsc] (2)

The compound **2** was prepared from 4-(*N*)-methylthiosemicarbazide (0.481g, 4.58 mmol) and 3-acetyl-8-methoxy-2H-chromen-2-one (1 g, 4.58 mmol) in the presence of glacial acetic acid. Single crystals suitable for X-ray diffraction studies were obtained by recrystallisation of **2** in methanol. Yield: 74 %. M.p: 114 °C. FT-IR (ν, cm^{-1}) in KBr: ν(C=O lactone) 1698, ν(C=N) 1613, ν (terminal -NH) 3278, ν(-NH) 3215, ν(C=S) 772. UV-Vis (DMSO), λ_{max} (ε): 268 (42,815) nm ($dm^3mol^{-1}cm^{-1}$); 343 (43,284) nm ($dm^3mol^{-1}cm^{-1}$). ^{1}H NMR (400 MHz, DMSO-d_6, δ ppm, *J* Hz): δ 8.33 (s, 1H, C4-H), δ 7.32-7.33 (m, 3H, Ar-H), δ 3.91 (s, 3H,-OCH_3), δ 2.23 (s, 3H,-CH_3), δ 10.44 (s, 1H, NH-C=S), δ 8.48-8.51 (q, 1H, terminal -NH), δ 3.00-3.01 (d, *J*=3.6, 1H, terminal –NH-CH_3).

Synthesis of ((1*E*)-1-(1-(8-methoxy-2-oxo-2H-chromen-3-yl)ethylidene) 4(*N*)-ethyl thiosemicarbazide) [8MAC-etsc] (3)

The compound **3** was prepared from 4-(*N*)-ethylthiosemicarbazide (0.546 g, 4.58 mmol) and 3-acetyl-8-methoxy-2H-chromen-2-one (1 g, 4.58 mmol) in the presence of glacial acetic acid. The compound was recrystallised by using methanol to yield suitable yellow crystals for X-ray analysis. Yield: 72 %. M.p: 176 °C. FT-IR (ν, cm^{-1}) in KBr: ν(C=O lactone) 1722, ν(C=N) 1615, ν (terminal -NH) 3278, ν(-NH) 3215, ν(C=S) 780. UV-Vis (DMSO), λ_{max} (ε): 252 (12,968) nm ($dm^3mol^{-1}cm^{-1}$); 316 (25,906) nm ($dm^3mol^{-1}cm^{-1}$). ^{1}H NMR (400 MHz, DMSO-d_6, δ ppm, *J* Hz): δ 8.30 (s, 1H, C4-H), δ 7.26-7.34 (m, 3H, Ar-H), δ 3.91 (s, 3H,-OCH_3), δ 2.23 (s, 3H,-CH_3), δ 10.32 (s, 1H, NH-C=S), δ 8.47-8.50 (t, *J*=5.6, 1H, terminal -NH), δ 3.55-3.60 (p, 2H, terminal –NH-CH_2), δ 1.11-1.15 (t, *J*=7.2, 3H, –CH_3).

Synthesis of ((1*E*)-1-(1-(8-methoxy-2-oxo-2H-chromen-3-yl)ethylidene) 4(*N*)-phenyl thiosemicarbazide) [8MAC-ptsc] (4)

The compound **4** was prepared from 4-(*N*)-phenylthiosemicarbazide (0.766 g, 4.58 mmol) and 3-acetyl-8-methoxy-2H-chromen-2-one (1 g, 4.58 mmol) in the presence of glacial acetic acid. Single crystals suitable for X-ray diffraction were obtained by recrystallisation of the compound in methanol and dichloromethane solution. Yield: 79 %. M.p: 180 °C. FT-IR (ν, cm^{-1}) in KBr: ν(C=O lactone) 1719, ν(C=N) 1602, ν (terminal -NH) 3281, ν(-NH) 3225, ν(C=S) 767. UV-Vis (DMSO), λ_{max} (ε): 276 (13,270) nm ($dm^3mol^{-1}cm^{-1}$); 331 (11,519) nm ($dm^3mol^{-1}cm^{-1}$). ^{1}H NMR (400 MHz, DMSO-d_6, δ ppm, *J* Hz): δ 8.47 (s, 1H, C3-H), δ 7.15-

7.59 (m, 8H, Ar-H), δ 3.91 (s, 3H,-OCH_3), δ 2.32 (s, 3H,-CH_3), δ 10.86 (s, 1H, NH-C=S), δ 10.15 (s, 1H, terminal -NH).

X-Ray crystallography

Suitable single crystals for the compounds **1-4** were obtained from methanol medium. Single crystal data collections and corrections for the compounds **1-4** were carried out with a Bruker kappa APEX-II DUO 1000 CCD diffractometer using graphite monochromated MoKα (λ= 0.71073 Å) radiation at 90.05 K and all the calculations were carried out by using SHELXS-97 [49] and SHELXL-2014/7 programs [50].

Biomolecular interaction and free radical scavenging studies

According to the methods described in our previous reports, we carried out the DNA binding, DNA viscosity studies, DNA cleavage experiments and albumin binding studies [51,52]. The DPPH radical scavenging assay [53] and total antioxidant activity of the compounds were determined by the literature methods [54].

***In vitro* antimicrobial studies**

Antimicrobial activities of the compounds were evaluated by agar well diffusion method [55] by taking various concentrations (25 µg/ml, 50 µg/ml and 100 µg/ml) of the compounds with different fungi (*A. niger, A. fumigatus, C. albicans, C. tropicalis and T. rubrum*) and bacteria (*S. aureus, S. paratyphi S. pneumonie and P. aeruginosa*).

Cytotoxicity studies

Anticancer activity of the compounds was examined with A549 (human lung cancer cells), MCF-7 (human breast cancer cell lines) and (HaCaT) human normal keratinocyte cells by using literature method [56]. The IC_{50} values were calculated from nonlinear regression by using GraphPad Prism 5 [57]. The NO release [58] and LDH release [59] assays of the compounds have been carried out by using methods of Stueher and Wacker respectively.

ACKNOWLEDGEMENT

The author G.K. greatly acknowledge **DST, New Delhi, India** for INSPIRE fellowship (IF140225 dated 23.01.2014). The author S.D greatly acknowledged **UGC, New Delhi, India** for UGC-BSR fellowship (F.25-1/2014-15(BSR)/7-26/2007(BSR) dated 05.11.2015).

References

1. K.V. Sashidhara, A. Kumar, M. Chatterjee, K.B. Rao, S. Singh, A.K. Verma, G. Palit, Bioorg. Med. Chem. Lett. 21 (2011) 1937.
2. M.A. Gouda, M.A. Berghot, E.A. Baz, W.S. Hamama, Med. Chem. Res. 21 (2012) 1062.
3. Y. Bansal, P. Sethi, G. Bansal, Med. Chem. Res. 22 (2013) 3049.
4. F. Chimenti, B. Bizzarri, A. Bolasco, D. Secci, P. Chimenti, A. Granese, S. Carradori, D. Rivanera, A. Zicari, M.M. Scaltrito, F. Sisto, Bioorg. Med. Chem. Lett. 20 (2010) 4922.
5. J.R. Hwu, S.Y. Lin, S.C. Tsay, E. De Clercq, P. Leyssen, J. Neyts, J. Med. Chem. 54 (2011) 2114.
6. X.M. Peng, G.L. Damu, C. Zhou, Curr. Pharm. Des. 19 (2013) 3884.
7. D. West, A. Liberta, S. Padhye, R. Chikate, P. Sonawane, A. Kumbhar, R. Yerande, Coord. Chem. Rev. 123 (1993) 49.
8. T. Okamoto, T. Kobayashi, Yoshida, Curr. Med. Chem. Anticancer Agents 5 (2005) 47.
9. A. Pankaj, D. Sanjib, A. Namita, G. Ashish, U.S. Baghel, Int. J. Pharm. Life Sci. 1 (2010) 113.
10. Y.Q. Hu, Z. Xu, S. Zhang, X. Wu, J.W. Ding, Z.S. Lv, L.S. Feng, Eur. J. Med. Chem. 136 (2017) 122.
11. T.G. Kraljevic, A. Harej, M. Sedic, S.K. Pavelic, V. Stepanic, D. Drenjancevic, J. Talapko, S. Raic-Malic, Eur. J. Med. Chem. 124 (2016) 794.
12. V. Pardo-Jiménez, C. Barrientos, K. Pérez-Cruz, P.A. Navarrete- Encina, C. Olea-Azar, L.J. Nuñez-Vergara, J.A. Squella, Electrochim. Acta 125 (2014) 457.
13. F. Borges, F. Roleira, N. Milhazes, L. Santana, E. Uriarte, Curr. Med. Chem. 12 (2005) 887.
14. K.C. Fylaktakidou, D.J. Hadjipavlou-Litina, K.E. Litinas, D.N. Nicolaides, Curr. Pharm. Des. 10 (2004) 3813.
15. L.R. Zacharski, W.G. Henderson, F.R. Rickles, W.B. Forman, C.J. Cornell Jr, R.J. Forcier, R.L. Edwards, E. Headley, S.H. Kim, J.F. O'Donnell, R. O'Dell, K. Tornyos, H.C. Kwaan, Cancer. 53 (1984) 2046.
16. A. Arshad, H. Osman, K.L. Chan, J.H. Goh, H.K. Fun, Acta Crystalographica. E66 (2010) o1491.
17. M. Adams, Y. Li, H. Khot, C. De Kock, P.J. Smith, K. Land, K. Chibale, G.S. Smith, Dalton Trans. 42 (2013) 4677.

18. P. Chellan, K.M. Land, A. Shokar, A. Au, S.H. An, C.M. Clavel, P.J. Dyson, C. De Kock, P.J. Smith, K. Chibale, G.S. Smith, Organometallics 31 (2012) 5791.
19. A. Moreno-Rodríguez, P.M. Salazar-Schettino, J.L. Bautista, F. Hernández-Luis, H. Torrens, Y. Guevara- Gómez, S. Pina-Canseco, M.B. Torres, M. Cabrera-Bravo, C.M. Martinez, E. Pérez-Campos, Eur. J. Med. Chem. 87 (2014) 23.
20. A. Walcourt, J. Kurantsin-Mills, J. Kwagyan, B.B. Adenuga, D.S. Kalinowski, D.B. Lovejoy, D.J.R. Lane, D.R. Richardson, J. Inorg. Biochem. 129 (2013) 43.
21. K.N. Anees Rahman, J. Haribabu, C. Balachandran, N.S.P. Bhuvanesh, R. Karvembu, A. Sreekanth, Polyhedron 135 (2017) 26.
22. G.R. Subhashree, J. Haribabu, S. Saranya, P. Yuvaraj, D. Anantha Krishnan, R. Karvembu, D. Gayathri, J. Mol. Struc. 1145 (2017) 160.
23. D.S. Ranade, A.M. Bapat, S.N. Ramteke, B.N. Joshi, P. Roussel, A. Tomas, P. Deschamps, P.P. Kulkarni, Eur. J. Med. Chem. 121 (2016) 803.
24. T. Pivetta, E. Valletta, G. Ferino, F. Isaia, A. Pani, S. Vascellari, C. Castellano, F. Demartin, M.G. Cabiddu, E. Cadoni, J. Inorg. Biochem. 177 (2017) 101.
25. W. Su, Q. Qian, P. Li, X. Lei, Q. Xiao, S. Huang, C. Huang, J. Cui, Inorg. Chem. 52 (2013) 12440.
26. G. Devagi, G. Shanmugam, A. Mohankumar, P. Sundararaj, F. Dallemer, P. Kalaivani, R. Prabhakaran, J. Organomet. Chem. 838 (2017) 12.
27. C. Umadevi, P. Kalaivani, H. Puschmann, S. Murugan, P.S. Mohan, R. Prabhakaran, J. Photochem. Photobiol. B: Biology 167 (2017) 45.
28. G. Micera, V.L. Pecoraro, E. Garribba, Inorg. Chem. 48 (2009) 5790.
29. N. Butenko, A.I. Tomaz, O. Nouri, E. Escribano, V. Moreno, S. Gama, V. Ribeiro, J.P. Telo, J. Costa Pessoa, I. Cavaco, J. Inorg. Biochem. 103 (2009) 622.
30. J. R. Lakowicz, Principles of Fluorescence Spectroscopy, third ed., Springer, US, 2006.
31. P. Kalaivani, S. Saranya, P. Poornima, R. Prabhakaran, F. Dallemer, V. Vijaya Padma, K. Natarajan, Eur. J. Med. Chem. 82 (2014) 584.
32. S. Mukhopadhyay, R.K. Gupta, R.P. Paitandi, N.K. Rana, G. Sharma, B. Koch, L.K. Rana, M.S. Hundal, D.S. Pandey, Organometallics 34 (2015) 4491.
33. K. Tsai, T.G. Hsu, K.M. Hsu, H. Cheng, T.Y. Liu, C.F. Hsu, C.W. Kong, Free Radical. Biol. Med. 31 (2001) 1465.
34. J. Haribabu, G. R. Subhashree, S. Saranya, K. Gomathi, R. Karvembu, D. Gayathri, J. Mol. Struc. 1094 (2015) 281.
35. K. Mahendra Raj, B.H.M. Mruthyunjayaswamy, J. Mol. Struc. 1074 (2014) 572.

36. R. Cini, G. Giorgi, A. Cinquantini, C. Rossi, M. Sabat, Inorg. Chem. 29 (1990) 5197.
37. S.K. Yusufzai, H. Osman, M. Shaheen Khan, S. Mohamad, O. Sulaiman, T. Parumasivam, J.A. Gansau, N. Johansah, Noviany, Med. Chem. Res. 26 (2017) 1139.
38. A. Arshad, H. Osman, M.C. Bagley, C. Kit Lam, S. Mohamad, A.S. Mohd Zahariluddin, Eur. J. Med. Chem. 46 (2011) 3788.
39. S. A. Patil, V.H. Naik, A.D. Kulkarni, P.S. Badami, Spectrochim. Acta Part A75 (2010) 347–354
40. A. Kulkarni, S.A. Patil, P.S. Badami, Eur. J. Med. Chem. 44 (2009) 2904.
41. M. B. Halli, R.B. Sumathi, Mallikarjun Kinni, Spectrochim. Acta Part A: Molecular and Biomolecular Spectroscopy 99 (2012) 46.
42. G. Kalaiarasi, Ruchi Jain, H. Puschman, S. Poorna Chandrika, K. Preethi, R. Prabhakaran, New. J. Chem. 41 (2017) 2543.
43. K. Jeyalakshmi, J. Haribabu, N.S.P. Bhuvanesh, R. Karvembu, Dalton Trans. 45 (2016) 12518.
44. a) C. Legrand, J.M. Bour, C. Jacob, J. Capiaumont, A. Martial, A. Marc, M. Wudtke, G. Kretzmer, C. Demangel, D. Duval, J. Hache, J. Biotechnol. 25 (1992) 231. b) E. Bonfoco, D. Krainc, M. Ankarcrona, P. Nicotera and S.A. Lipton, Proc. Natl. Acad. Sci. U. S. A. 16 (1995) 7162.
45. R. Prabhakaran, P. Kalaivani, R. Huang, P. Poornima, V. Vijaya Padma, F. Dallemer, K. Natarajan, J. Biol. Inorg. Chem. DOI 10.1007/s00775-012-0969-x
46. L. Yu, P.E. Gengaro, M. Niederberger, T.J. Burke, R.W. Schriert, Proc. Natl. Acad. Sci. U.S.A. 91 (1994) 1691.
47. A.I. Vogel, Textbook of Practical Organic Chemistry, 5 th ed., Longman, London, 1989, 268.
48. M. S. Refat, I. M. El-Deen, Z. M. Anwer, S. El-Ghol, J. Mol. Struc. 920 (2009) 149.
49. G.M. Sheldrick, SHELXL-97, Program for Structure Refinement, University of Gottingen, Gottingen, Germany, 1997.
50. G.M. Sheldrick, SHELXL-2014/7: Program for the Solution of Crystal Structures, University of Gottingen, Gottingen, Germany, 2014.
51. G. Kalaiarasi, S. Rex Jeya Rajkumar, S. Dharani, V.M. Lynch, R. Prabhakaran, Inorg. Chim. Acta 471 (2018) 759.
52. G. Kalaiarasi, S. Rex Jeya Rajkumar, S. Dharani, F.R. Fronczek, M.S.A. Muthukumar Nadar, R. Prabhakaran, New. J. Chem. 42 (2018) 336.
53. M.S. Blios, Nature 29 (1958) 1199.

54. P. Prieto, M. Pineda, M. Aguilar, Analytical Biochemistry 269 (1999) 337.
55. I. Weigand, K. Hilpert, R.E.W. Hancock, Nature Protocols 3 (2008) 163.
56. T.J. Mossman, Immunol. Methods 65 (1983) 55.
57. H.J. Motulsky, Prism 5 Statistics Guide, GraphPad Software Inc., San Diego, CA, 2007, http://www.graphpad.com.
58. D.J. Stueher, M.A. Marletta, J. Immunol. 139 (1987) 518.
59. W.E.C. Wacker, D.D. Ulmer, B.L. Vallee, J. Med. Chem. 255 (1956) 449.

Graphical abstract

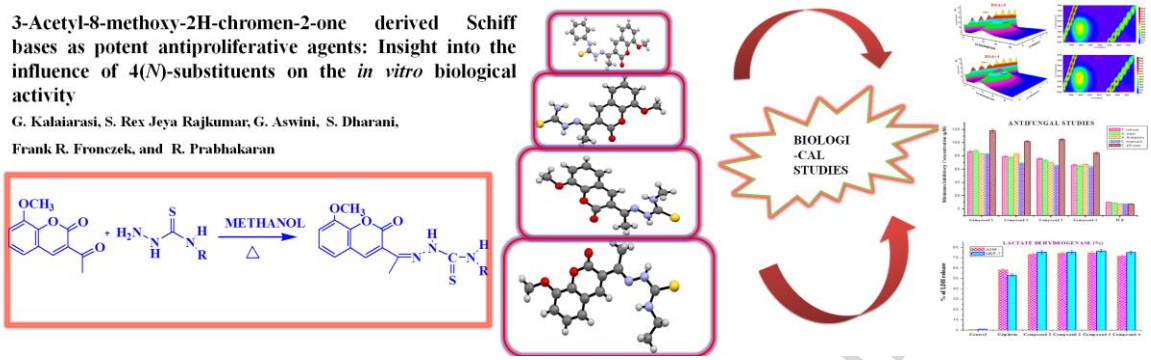

HIGHLIGHTS

- 8-methoxy-3-acetyl-coumarin derived Schiff bases were synthesized and characterized
- DNA/protein interactions of the compounds were studied by a variety of techniques
- Antimicrobial activity against bacterial and fungal pathogens have been examined
- The antiproliferative activity was evaluated against MCF-7 and HeLa cell lines
- The compounds showed potent anticancer activity over the standard drug, *Cisplatin*
- Assay on HaCaT cell lines showed that the compounds were non-toxic to those cells.